



Approximating Riemann-Stieltjes Integral Using New Time and Cost Efficient Trapezoid-Type Quadrature

Kashif Memon¹, Muhammad Mujtaba Shaikh², Sara Mahesar², Kamran Malik³, Hijaz Ahmad^{4,5,6,*}, Berna Uzun⁴, Ilker Ozsahin^{4,7}, Waleed Mohammed Abdelfattah^{8,9}

¹ Institute of Mathematics and Computer Science, University of Sindh, Jamshoro, Sindh, Pakistan

² Department of Basic Sciences and Related Studies, Mehran University of Engineering and Technology, Jamshoro, Sindh, Pakistan

³ Department of Mathematics, Government College University, Hyderabad, Pakistan

⁴ Operational Research Center in Healthcare, Near East University, Nicosia/TRNC, 99138 Mersin 10, Turkey

⁵ Sustainability Competence Centre, Széchenyi István University, Egyetem tér 1, H-9026 Győr, Hungary

⁶ Department of Mathematics, College of Science, Korea University, 145 Anam-ro, Seongbuk-gu, Seoul 02841, South Korea

⁷ Department of Mathematical Sciences, Saveetha School of Engineering, SIMATS, Chennai, Tamilnadu, India

⁸ College of Engineering, University of Business and Technology, Jeddah 23435, Saudi Arabia

⁹ Department of Engineering Mathematics and Physics, Faculty of Engineering, Zagazig University, P.O. 44519, Egypt

Abstract. Engineers and scientists adopt numerical integration to achieve an approximate solution for definite integrals that have no analytic solution. This research focuses on developing some new derivative-based quadrature schemes for numerically integrating the integral of Riemann-Stieltjes (Rs-integral) by proposing new schemes which are based on trapezoid-type quadrature. The process of undetermined coefficients has been used for the derivation of proposed schemes. The theoretical derivation and numerical verification of orders of accuracy have been addressed in line with the degrees of precision, and a sufficient improvement has been demonstrated over the existing schemes. The theorems regarding single and multiple use of the suggested schemes in a finite interval have been proved along with the theoretical results on residual terms, both locally and globally. All suggested schemes have been verified to reduce to corresponding variants for the Riemann integral in the case when integrator $g(t) = t$. Numerical experiments have been performed on all the discussed schemes with the help of MATLAB coding. The experimental results assure the smaller numerical errors by the proposed schemes in the comparison of existing schemes. The obtained results show the efficiency of proposed schemes in light of computational burden and CPU time (in seconds) with reference to the existing quadrature. The proposed work substantially advances the existing knowledge with an addition of derivative-based correction terms in the usual quadrature in a way that the consequent computational costs and execution times are also minimized.

2020 Mathematics Subject Classifications: 65D30, 65D32

Key Words and Phrases: Quadrature rule, Riemann-Stieltjes integral, trapezoidal rule, derivative-based schemes, midpoint methods, means

*Corresponding author.

DOI: <https://doi.org/10.29020/nybg.ejpam.v18i4.7112>

Email addresses: hijaz.ahmad@neu.edu.tr (H. Ahmad)

1. Introduction

One of the oldest and most attractive concepts in numerical analysis is numerical integration. When integrating $f(x)$ analytically is difficult or impossible, or if the values of $f(x)$ are defined in tabular form, then the numerical integration methods are applied. However, numerical integration gives only the approximate value of the integral with given parameters. Numerical integration generates better results when it is solved properly with appropriate methods. The term quadrature is used to describe numerical integration in one dimension. Quadrature formulas are usually based on polynomial interpolation. Mostly, the conventional Newton-Cotes quadrature formulae work well for definite integrals. Different types of Newton-Cotes formulas are known that are based on the range of the limits a and b . The Newton-Cotes formulae of closed type, which include both endpoints, can be regarded as a bulk of essential formulas. The closed Newton-Cotes integration formulae include the Trapezoid rule as a specific case. The integrand function is fitted with n th degree polynomials at $n + 1$ control points to obtain this formula. Mostly, attention of research works in the field of numerical integration was focused on the Riemann integral. Similar progress may be achieved for the RS-integral. The evaluation of RS-integral, in which the integrand is $f(x)$ and the integrator is another function of x , $\alpha(x)$, develops a mainstream part in mathematics [1]. RS-integral may be applied in the areas of statistics and probability theory of operators, mathematical analysis, etc. Obviously, the RS-integral can be regarded as an enhancement of the usual integration by Riemann, in a way that besides the integrand f , the integrator also depends on x . While a considerable effort in literature has been done on enhancing quadrature rules for the classical Riemann integrals as compared to the RS-integrals, only some investigations have been attempted to approximate the RS-integral. In 2008, Mercer [2] offered the Trapezoidal rule extension which addressed the applicability of the Hadamard integral inequality for the RS-integral. Moreover, in 2012, Mercer [3] introduced a new approach for midpoint and Simpson's schemes on the RS-integral, based on the concept of relative convexity. In 2013, Zhao and Li [4] developed a novel midpoint derivative-based family of closed Newton-Cotes quadrature rules. Afterwards in 2014, Zhao et al. [5] proposed a trapezoid rule for the RS-integral based on the midpoint derivative, in which the function derivative was computed using the midpoint. In 2016, Shaikh et al. [6] improved with the second-order derivative-based rule with the help of midpoint, the Zhao and Li's [4] scheme of Simpson's 3/8-type, which had used fourth-order derivative.

There are so many works that have been done on the numerical enhancement of the usual integration formulas of Newton and Cotes. In 2016, Ramachandran et al. [7] developed a novel quadrature of the closed form that used the geometric mean value to compute the derivative. They proved that this novel quadrature scheme provided an improvement of a single order in precision against the traditional closed quadrature by Newton and Cotes. In 2016, Ramachandran et al. [8] developed another closed-form novel quadrature approach that used the harmonic mean value to compute the derivative. They proved that this novel quadrature scheme provided an improvement of a single order in precision over the closed Newton-Cotes quadrature formula. Ramachandran et al. [9] performed a test

among three derivative-based closed Newton-Cotes quadrature schemes which were proposed in [4, 7, 8]. According to the comparison, the arithmetic mean derivative-based rule was much more effective than the other schemes. Moreover, Ramachandran et al. [10]-[11] developed the closed Newton-Cotes scheme to evaluate function derivatives using heronian mean and centroidal mean. They proved that these novel quadrature schemes provide an improvement of a single order in precision over the closed Newton-Cotes quadrature formula. The work in [12] encouraged proposition of time and cost effective quadrature schemes by utilizing derivative corrections as a better and efficient way to enhance the accuracy and precision of Riemann integral approximations as well. In recent years, some work has been focused on the approximation of RS-integral using different means, but with more nodal points in the sense of Simpson's quadrature, for example [13], [14] and [15]. The applications of the RS-integral can be further studied through [16], whereas the studies [17] and [18] provide a way forward to apply the numerical procedures in the mesh-free sense to better deal with some case studies in engineering science.

This research extends some recent derivative-based quadrature schemes of the Riemann integral into corresponding efficient derivative-based quadrature schemes for the RS-integral using different means. Further, the suggested schemes include the work of Zhao et al. [5] for the RS-integral with modification. The suggested schemes are much more effective than the Zhao et al. [5] scheme in comparison. The composite form is involved for the purpose of reducing errors. The derivations of suggested schemes are proved in composite form for the RS-integral and used for the numerical experiments. Finally, the theoretical and numerical results tailor the time and cost effectiveness of the proposed quadrature in terms of standard parameters, like: absolute error, cost, and CPU times.

2. Materials and Methods

2.1. Basics of Riemann and Riemann-Stieltjes integrals and their existing quadrature

For integrating a function $f(x)$ from $x = a$ to $x = b$, the basic Riemann notation is:

$$I(f; a, b) = \int_a^b f(x) dx \quad (1)$$

Geometrically, $I(f; a, b)$ represents area bounded between $f(x)$ and X-axis when x varies from a to b . The RS-integral advances the Riemann concept of integration, which was limited to integrating a function $f(x)$ in a segment of the set of real numbers. The RS-integral utilizes integrator which is another function of x , and also monotonic rising but bounded. Therefore, it is important to frame and analyze the latter instance geometrically in three dimensions. The RS-integral notation can be describes as:

$$RS(f; g; a, b) = \int_a^b f(t) d\alpha(t) \quad (2)$$

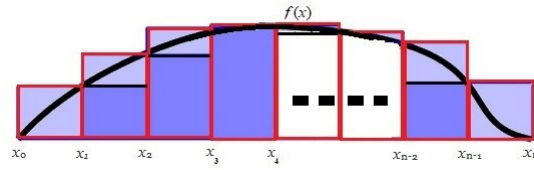


Figure 1: Geometrical representation of Riemann integral

where integrator is increasing there with both continuous integrand and integrator in the interval of integration. The width of a sub-rectangle can be computed by differences in the precise values of x in that sub-interval, which are the interval's end points in the Riemann integral. However, the similar partitioning is done using the differences in the integrator increasing function's values in the RS-integral. The geometrical form of the Riemann integral is shown in Fig. 1, where the x -axis is used to divide the area into rectangles, and limiting case of areas summed-up define the integral. The similar explanation on the RS-integral is explained in Fig.2. The graphs of integrator and integrand can be seen initially in 2D plane, each versus the X -axis, and then the rectangular regions that cover the surface area using the RS-integral are identified on the three-dimensional graph.

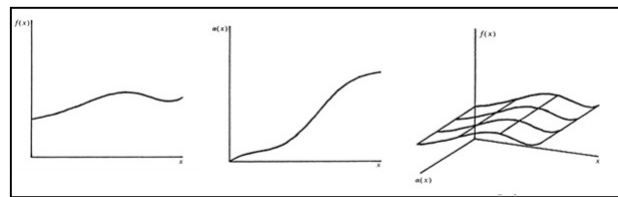


Figure 2: Geometrical representation of Riemann-Stieltjes integral [19]

The Riemann notion of integral $I(f; a, b)$ through (1), when evaluated numerically using a quadrature scheme, is the sum of products of the integrand evaluated at some finite discrete points and the corresponding weights. We can write with reference to [1]:

$$I(f; a, b) = \int_a^b f(x) dx \approx \sum_{i=0}^n w_i f(x_i) \quad (3)$$

The quantities w_i and $x_i = a + ih$ are, respectively, the weights and abscissas/nodes, where $h = \frac{b-a}{n}$ and the index i varies from 0 to n . The nodes can be the equally-spaced points in the interval of integration – as the case of widely used quadrature by Newton and Cotes – or also zeros of orthogonal polynomials in the sense of quadrature introduced by Gauss. The most basic techniques are the Newton-Cotes quadrature formulas. The closed Newton-Cotes quadrature formulas include the end points of integration interval $[a, b]$ for evaluating the integral that is described as:

$$I(f; a, b) = \int_a^b f(x) dx \approx \sum_{i=0}^n w_i f(x_0 + ih) \quad (4)$$

There are several methods for calculating the weighting coefficients in equation (4). One basic approach of a quadrature formula is concerned with the precision, in which the weight values w_0, w_1, \dots, w_n are considered to have a zero approximation error in equation (4), i.e.

$$E(f) = \int_a^b f(x) dx - \sum_{i=0}^n w_i f(x_i) = 0 \quad (5)$$

where $f(x)$ are monic polynomials, where degree j varies from 0 to n .

A few important metrics related to accuracy and errors associated to quadrature rules are explained here for accommodating better understanding of the forthcoming sections.

Definition 1. If a quadrature formula is able to exactly integrate all polynomials of degree up to n , but not onward, then we say that it has a degree of exactness/precision of n .

Definition 2. Order of accuracy of a quadrature formula refers to the exponent of the truncation error term, and it indicates decrease of error as step-size decreases.

Definition 3. General truncation error in a quadrature rule which has degree of exactness of p can be expressed as:

$$R[f] = Ch^{(p+1)} f^{(p+1)}(\epsilon) \quad (6)$$

where c is a nonzero constant, h is the width of interval and $p + 1$ is the order of error term with precision p . Listed below are a few recognized members of the closed-form quadrature by Newton and Cotes for approximating Riemann integration [1] with local approximations and truncation errors:

$$\int_a^b f(x) dx = \frac{b-a}{2} [f(a) + f(b)] - \frac{(b-a)^3}{12} f''(\xi) \quad (7)$$

$$\int_a^b f(x) dx = \frac{b-a}{6} \left[f(a) + 4f\left(\frac{a+b}{2}\right) + f(b) \right] - \frac{(b-a)^5}{2880} f^{(4)}(\xi) \quad (8)$$

$$\int_a^b f(x) dx = \frac{b-a}{8} \left[f(a) + 3f\left(\frac{2a+b}{3}\right) + 3f\left(\frac{a+2b}{3}\right) + f(b) \right] - \frac{(b-a)^5}{6480} f^{(4)}(\xi) \quad (9)$$

where $\xi \in (a, b)$. The precision of the Trapezoidal rule is 1, and its order of accuracy is 2, as it gives an exact proper integral of polynomials of degree one or less. The precision of the Simpson's 3-point (1/3) rule is 3, and its order of accuracy is 4, as it gives an exact proper integral of polynomials of degree three or less. The rule (9) has same precision 3 as of (8), and order of accuracy 4. Besides the usual closed-form rules by Newton and Cotes, there exist quadrature proposed in last decade which use derivatives and correction terms in the usual closed-form rules [4], [7], [8], [10], [11]. Here, we refer to the local approximations and truncation error terms of such quadrature. The arithmetic mean derivative-based Trapezoidal rule [4] has exactness degree of 3, and is described as:

$$\int_a^b f(t) dt = \frac{b-a}{2} [f(a) + f(b)] - \frac{(b-a)^3}{12} f''\left(\frac{a+b}{2}\right) - \frac{(b-a)^5}{480} f^{(4)}(\xi), \quad (10)$$

The geometric mean derivative-based Trapezoidal rule [7] with degree of exactness 2 is described as:

$$\int_a^b f(t) dt = \frac{b-a}{2} [f(a) + f(b)] - \frac{(b-a)^3}{12} f''(\sqrt{ab}) - \frac{(b-a)^3}{24} (\sqrt{b} - \sqrt{a})^2 f^{(3)}(\xi), \quad (11)$$

The harmonic mean derivative-based Trapezoidal rule [8] with degree of exactness 2 is described as:

$$\int_a^b f(t) dt = \frac{b-a}{2} [f(a) + f(b)] - \frac{(b-a)^3}{12} f''\left(\frac{2ab}{a+b}\right) - \frac{(b-a)^5}{24(a+b)} f^{(4)}(\xi), \quad (12)$$

The heronian mean derivative-based Trapezoidal rule [10] with degree of exactness 2 is described as:

$$\int_a^b f(t) dt = \frac{b-a}{2} [f(a) + f(b)] - \frac{(b-a)^3}{12} f''\left(\frac{a + \sqrt{ab} + b}{3}\right) - \frac{(b-a)^3}{72} (\sqrt{b} - \sqrt{a})^2 f^{(3)}(\xi), \quad (13)$$

The centroidal mean derivative-based Trapezoidal rule [11] with degree of exactness 2 is described as:

$$\int_a^b f(t) dt = \frac{b-a}{2} [f(a) + f(b)] - \frac{(b-a)^3}{12} f''\left(\frac{2(a^2 + ab + b^2)}{3(a+b)}\right) + \frac{(b-a)^5}{72(a+b)} f^{(4)}(\xi), \quad (14)$$

One can note that the formula (10) can be said, comparatively in contrast with others (11)-(14), to have no limitations on the choice of limits of integration. On the other hand, methods (11)-(14), are prone to limitations based on the limits of integration. For example, (11) and (13) lead to complex number arithmetic if limits of integration are opposite in sign. In this way, (12) and (14) lead to indeterminate and undefined forms when limits of integration add up to zero. It should also be noted that the * in (12) and (14) refers to the studies [8] and [11], respectively, where authors put fourth-order derivative in the error term, whereas it is expected that an interpolatory quadrature has $(p+2)^{nd}$ order derivative in the local error term if its precision is p.

The extension of the conventional Trapezoid rule of the Riemann integral is discussed in [20] for the approximation of RS-integral. So, its resulting conventional Trapezoid rule without derivative for RS integral with local error term is as follows:

$$\begin{aligned} RS(f; g; \alpha, \beta) &= \int_{\alpha}^{\beta} f(x) dg = T + R_T[f] = \left(\frac{1}{\beta - \alpha} \int_{\alpha}^{\beta} g(t) dt - g(\alpha) \right) f(\alpha) \\ &\quad + \left(g(\beta) - \frac{1}{\beta - \alpha} \int_{\alpha}^{\beta} g(t) dt \right) f(\beta) - \frac{(\beta - \alpha)^3}{12} f''(\xi) g'(\eta), \quad (15) \end{aligned}$$

where $\xi, \eta \in (\alpha, \beta)$

The rule (15) describes the formula of two points, so its performance of large integration intervals is not appropriate. In order to get smaller local errors in each approximation, the composite scheme of original Trapezoid rule, referred here as CT scheme with global error term, for RS integrals given in [20] is:

$$\begin{aligned} \int_{\alpha}^{\beta} f(t) dg = CT + R_{CT}[f] &= \left[\frac{\eta}{\beta - \alpha} \int_{\alpha}^{x_1} g(t) dt - g(\alpha) \right] f(\alpha) \\ &+ \frac{\eta}{\beta - \alpha} \sum_{k=1}^{n-1} \left[\int_{x_k}^{x_{k+1}} g(t) dt - \int_{x_{k-1}}^{x_k} g(t) dt \right] f(x_k) \\ &+ \left[g(\beta) - \frac{\eta}{\beta - \alpha} \int_{x_{n-1}}^{\beta} g(t) dt \right] f(\beta) - \frac{(\beta - \alpha)^3}{12n^2} f''(\mu)g''(\eta), \quad (16) \end{aligned}$$

where, $\mu, \eta \in (\alpha, \beta)$

Zhao et al. [21] discussed the conventional Trapezoidal rule with the midpoint derivative for the RS integral. So, its resulting scheme is as follows:

$$\int_a^{\beta} f(x) dg \approx ZT = T + \left(\int_a^{\beta} \int_a^t g(x) dx dt - \frac{\beta - a}{2} \int_a^{\beta} g(t) dt \right) f''(c), \quad (17)$$

where,

$$c = \frac{(-2\beta^2 + \alpha^2 - \alpha\beta) \int_{\alpha}^{\beta} g(t) dt + 6\beta \int_{\alpha}^{\beta} \int_{\alpha}^t g(x) dx dt - 6 \int_{\alpha}^{\beta} \int_{\alpha}^t \int_{\alpha}^y g(x) dx dy dt}{6 \int_{\alpha}^{\beta} \int_{\alpha}^t g(x) dx dt - 3(\beta - \alpha) \int_{\alpha}^{\beta} g(t) dt}, \quad (18)$$

This method has precision 3 and its error term $R[f]$ is as follows:

$$\begin{aligned} &\frac{\alpha^3 + \alpha\beta^2 + \alpha^2\beta^2 - 3\beta^3 + 6(\beta - \alpha)c^2}{24} \left[\int_{\alpha}^{\beta} g(t) dt + \frac{\beta^2 - \alpha^2}{2} \left(\int_{\alpha}^{\beta} \int_{\alpha}^t g(x) dx dt \right) \right. \\ &\quad \left. - \beta \int_{\alpha}^{\beta} \int_{\alpha}^t \int_{\alpha}^y g(x) dx dt + \int_{\alpha}^{\beta} \int_{\alpha}^t \int_{\alpha}^z \int_{\alpha}^y g(x) dx dy dz dt \right] f^{(4)}(\xi), \quad (19) \end{aligned}$$

where $\xi \in (\alpha, \beta)$ While in [5] Zhao et al. attempted to modify the existing trapezoid-type scheme without derivatives by introducing derivative of second-order at point c , the improvement happens to be quite complicated and demands a lot of computational effort due to complicated formula of c in the complete formula. Further, in scheme (17), when $g(t) = t$, then expression of c reduces to $\frac{(\alpha+\beta)^3}{2(\alpha-\beta)^2}$ instead of $\frac{(\alpha+\beta)}{2}$. Consequently, the scheme of Zhao et al. [5] was rectified by modified Zhao Trapezoidal rule (MZT) in [22]. The MZT scheme is:

$$\int_a^\beta f(x) dg \approx MZT = \left(\frac{1}{\beta - a} \int_a^\beta g(t) dt - g(a) \right) f(a) + \left(g(\beta) - \frac{1}{\beta - a} \int_a^\beta g(t) dt \right) f(\beta) \\ + \left(\int_a^\beta \int_a^t g(x) dx dt - \frac{\beta - a}{2} \int_a^\beta g(t) dt \right) f''(c), \quad (20)$$

where

$$c = \frac{(-2\beta^2 + \alpha^2 + \alpha\beta) \int_a^\beta g(t) dt + 6\beta \int_a^\beta \int_a^t g(x) dx dt - 6 \int_a^\beta \int_a^t \int_a^y g(x) dx dy dt}{6 \int_a^\beta \int_a^t g(x) dx dt - 3(\beta - \alpha) \int_a^\beta g(t) dt}, \quad (21)$$

This MZT method has precision 3 and its error term $R[f]$ is as follows:

$$\frac{\alpha^2 + \alpha\beta^2 + \alpha^2\beta - 3\beta^3 + 6(\beta - \alpha)c^2}{24} \left(\int_a^\beta g(t) dt + \frac{\beta^2 - c^2}{2} \left[\int_a^\beta \int_a^t g(x) dx dt \right. \right. \\ \left. \left. - \beta \int_a^\beta \int_a^t \int_a^y g(x) dx dy dt + \int_a^\beta \int_a^t \int_a^x \int_a^y g(x) dx dy dz dt \right] f^{(4)}(\xi) \right), \quad (22)$$

where, $\xi \in (\alpha, \beta)$

2.2. Proposed Trapezoid-type quadrature for approximating Riemann-Stieltjes integral

The main motivation in the present study lies on proposing time and cost efficient trapezoid-type quadrature basing the contributions around the simplicity of c in the formula introduced in [5]. Because of the complicated c in (17), its dependence on the integrand and integrator functions, its dependence on derivatives of integrator and integrals of integrator, it is imperative to think of precise and simple c in (17). In this attempt, we consider the analogies from recent advancements in the case of Riemann integrals where the derivatives were used in addition to the actual trapezoid approximations to enhance the accuracy [4], [7], [8], [10], [11]. The points at which derivatives were used in these studies were statistical averages of the limits of the interval of integration. Selecting such means in the proposed trapezoid-type quadrature for the RS-integral to evaluate derivatives in advance minimizes the computational cost and execution times, without compromising on the accuracy of the quadrature. It will be demonstrated that our enhancements prove to be efficient than those suggested and used on this subject through [5] and [22]. The contributions are divided in two sections here: firstly we derive and prove theorems on the proposed trapezoid-type quadrature using arithmetic mean, and secondly the similar discussion is precisely extended to other averages.

2.2.1. Approximating Riemann-Stieltjes integral using arithmetic mean trapezoid-type quadrature

In the formula (17), we restrict c to be the mid-point of the limits of integration, or in other words, arithmetic average of the limits, then consequent trapezoid-type approximation so obtained is referred as AMT, and the quadrature is derived in Theorem 1.

Theorem 1. Assuming continuity of $f(t)$ and $g(t)$ in along with $g(t)$ being monotonically rising in the same interval, AMT quadrature for the RS-integral is:

$$\int_{\alpha}^{\beta} f(t) dg \approx AMT = \left(\frac{1}{\beta - \alpha} I_1 - g(\alpha) \right) f(\alpha) + \left(g(\beta) - \frac{1}{\beta - \alpha} I_1 \right) f(\beta) + \left(I_2 - \frac{\beta - \alpha}{2} I_1 \right) f' \left(\frac{\alpha + \beta}{2} \right), \quad (23)$$

where

$$I_1 = \int_{\alpha}^{\beta} g(t) dt, \quad I_2 = \int_{\alpha}^{\beta} \int_{\alpha}^t g(x) dx dt, \quad I_3 = \int_{\alpha}^{\beta} \int_{\alpha}^t \int_{\alpha}^y g() dx dy dt, \quad \text{and} \\ I_4 = \int_{\alpha}^{\beta} \int_{\alpha}^t \int_{\alpha}^z \int_{\alpha}^y g(x) dx dy dz dt.$$

Proof. Referencing to the AMT scheme for the Riemann integral as in [4], the proposed AMT quadrature for the RS-integral can be described generally as:

$$\int_{\alpha}^{\beta} f(t) dg \approx a_0 f(\alpha) + b_0 f(\beta) + c_0 f' \left(\frac{\alpha + \beta}{2} \right). \quad (24)$$

Looking at the precision of (1) [4], we can expect the degree of exactness of (24) to be 3 as well. AMT quadrature in (24) when integrand is allowed to be a monomial of degree at most 3 leads to four equations:

$$\int_{\alpha}^{\beta} 1 dg = a_0 + b_0, \\ \int_{\alpha}^{\beta} t dg = a_0 \alpha + b_0 \beta, \\ \int_{\alpha}^{\beta} t^2 dg = a_0 \alpha^2 + b_0 \beta^2 + 2c_0, \\ \int_{\alpha}^{\beta} t^3 dg = a_0 \alpha^3 + b_0 \beta^3 + 3c_0(\alpha + \beta).$$

The following system of equations (25)-(29) has been obtained using the integration technique by parts of the RS integral.

$$a_0 + b_0 = g(\alpha) + (\beta), \quad (25)$$

$$a_0 \alpha + b_0 \beta = \frac{\alpha}{\beta - \alpha} I_1 - \alpha g(\alpha) + \beta g(\beta) - \frac{\beta}{\beta - \alpha} I_1$$

$$\Rightarrow a_0 \alpha + b_0 \beta = \beta g(\beta) - \alpha g(\alpha) - I_1 \quad (26)$$

$$a \alpha^2 + b \beta^2 + 2c_0 = \left(\frac{\alpha^2}{\beta - \alpha} - \frac{\beta^2}{\beta - \alpha} \right) I_1 - \alpha z^2 g(\alpha) + \beta^2 g(\beta) + 2I_1 - (\beta - \alpha)^2 I_1 \quad (27)$$

$$\Rightarrow a \alpha^2 + b_0 \beta^2 + 2c_0 = \beta^2 g(\beta) - 2\beta I_1 + 2I_2 \quad (28)$$

$$a_0 \alpha^3 + b_0^2 \beta^3 + 3c_0(\alpha + \beta) = \frac{\alpha^3}{\beta - \alpha} I_1 - \alpha^3 g(\alpha) - \beta^3 g(\beta) - \frac{\beta^3}{\beta - \alpha} I_1 + 3(\alpha + \beta) I_2 - \frac{3}{2}(\beta^2 - \alpha^2) I_1$$

$$\Rightarrow a_0 \alpha^3 + b_0 \beta^3 + 3c_0(\alpha + \beta) = \beta^3 g(\beta) - \alpha^3 g(\alpha) - 3\beta^2 I_1 + 6\beta I_2 - 6I_3 \quad (29)$$

The following matrix is obtained from the system of linear equations (25)-(29) in the unknowns:

$$M = \begin{bmatrix} 1 & 1 & 0 \\ \alpha & \beta & 0 \\ \alpha^2 & \beta^2 & 2 \\ \alpha^3 & \beta^3 & 3(\alpha + \beta) \end{bmatrix}$$

The above matrix M is further written in reduced row echelon form as:

$$M \approx M_R = \begin{bmatrix} 1 & 0 & 0 \\ 0 & 1 & 0 \\ 0 & 0 & 1 \\ 0 & 0 & 0 \end{bmatrix}$$

It is observed from M_R that the $\text{rank}(M) = 3$, since the reduced row echelon form has three nonzero rows. So, we solve the above equations (25), (26), and (28) simultaneously to determine the coefficients a_0, b_0 and c_0 .

$$\begin{aligned} a_0 &= \frac{1}{\beta - \alpha} I_1 g(\alpha) \\ b_0 &= g(\beta) - \frac{1}{\beta - \alpha} I_1 \\ c_0 &= \left(\frac{\beta - \alpha}{2}\right) I_1 + I_2 \end{aligned}$$

Putting the values of coefficients a_0, b_0 and c_0 in (24), we have:

$$\int_{\alpha}^{\beta} f(t) dg \approx \left[\frac{1}{\beta - \alpha} I_1 - g(\alpha) \right] f(\alpha) + \left[g(\beta) - \frac{1}{\beta - \alpha} I_1 \right] f(\beta) + \left[\left(\frac{\beta - \alpha}{2}\right) I_1 + I_2 \right] f' \left(\frac{\alpha + \beta}{2} \right). \quad (30)$$

This formula is the required AMT quadrature, as in (23).

Theorem 2 presents truncation error in the AMT quadrature locally.

Theorem 2. Assuming continuity of $f(t)$ and $g(t)$ in along with $g(t)$ being monotonically rising in the same interval $[\alpha, \beta]$, AMT quadrature's truncation error for the RS-integral is:

$$\begin{aligned} R_{AMT}[f] &= \left(\frac{2\alpha^3 + 2\alpha\beta^2 - 6\beta^3 + 3(\beta - \alpha)(\alpha + \beta)^2}{48} I_1 \right) f^{(4)}(\xi) g(\eta) \\ &\quad + \left(\frac{4\beta^2 - (\alpha + \beta)^2}{8} I_2 - I_2 \beta I_3 + I_4 \right) f^{(4)}(\xi) g(\eta) \quad (31) \end{aligned}$$

Proof. Taking for the truncation error, as degree of exactness of (23) is 3, we have:

$$R_{AMT}[f] = \frac{1}{4!} \int_{\alpha}^{\beta} t^4 dg - AMT(t^4; g; \alpha, \beta) \quad (32)$$

From [4], we know that:

$$\frac{1}{4!} \int_{\alpha}^{\beta} t^4 dg = \frac{1}{24} ((\beta^4 g(\beta)) - \alpha^4 g(\alpha)) - \frac{\beta^3}{6} I_1 - \beta I_3 + I_4 \quad (33)$$

By Theorem 1 and scheme (23), we have:

$$AMT(t^4; g; \alpha, \beta) = \frac{\alpha^2}{4!} \left(\frac{1}{\beta - \alpha} I_1 - g(\alpha) \right) + \frac{\beta^2}{4!} \left(g(\beta) - \frac{1}{\beta - \alpha} I_1 \right) \\ + \frac{(\alpha + \beta)^2}{8} \left(I_2 - \frac{\beta - \alpha}{2} I_1 \right) \frac{1}{2!} \left(\frac{\alpha + \beta}{2} \right)^2 \quad (34)$$

$$R_{AMT}[f] = \frac{1}{24} [(\beta^4 g(\beta) - \alpha^4 g(\alpha)) - \frac{(\beta)^3}{6} I_1 + \frac{(\beta)^2}{2} I_2 - \beta I_3 + I_4 + \frac{\alpha^4}{24(\beta - \alpha)} I_1 + \frac{\alpha^4 g(\alpha)}{24} \\ - \frac{\beta^4 g(\beta)}{24} + \frac{\beta^4}{24(\beta - \alpha)} I_1 - \frac{(\alpha + \beta)^2}{8} I_2 + \frac{(\beta - \alpha)(\alpha + \beta)^2}{16}] f^{(4)}(\xi) g(\eta) \quad (35)$$

$$R_{AMT}[f] = \left(\frac{2\alpha^3 + 2\alpha\beta^2 + 2\alpha^2\beta - 6\beta^3 + 3(\beta - \alpha)(\alpha + \beta)^2}{48} \right) I_1 \\ + \left[\frac{4\beta^2 - (\alpha - \beta)^2}{8} I_2 - \beta I_3 + I_4 \right] f^{(4)}(\xi) g(\eta) \quad (36)$$

Theorem 3. If $g(t) = t$, then AMT quadrature and its truncation error term as in (23)-(24) for RS integral reduces to simple AMT quadrature (10) [4].

Proof. Obtaining the following using the Theorem 2:

$$\int_a^\beta f(t) dg \\ = \int_a^\beta f(t) dt = \left(\frac{1}{\beta - \alpha} \int_a^\beta t dt - g(\alpha) \right) f(\alpha) + \left(g(\beta) - \frac{1}{\beta - \alpha} \int_a^\beta t dt \right) f(\beta) \\ + \left(\int_a^\beta \int_a^t x dx dt - \frac{\beta - \alpha}{2} \int_a^\beta t dt \right) f'' \left(\frac{\alpha + \beta}{2} \right) \\ + \frac{2\alpha^3 + 2\alpha\beta^2 + 2\alpha^2\beta - 6\beta^3 + 3(\beta - \alpha)(\alpha + \beta)^2}{48} \int_a^\beta t dt \\ + \frac{4\beta^2 - (\alpha + \beta)^2}{8} \left(\int_a^\beta \int_a^t x dx dt - \beta \int_a^\beta \int_a^t \int_a^y x dx dy dz \right) f^{(4)}(\xi) g'(\eta) \\ + \left(\int_a^\beta \int_a^t \int_a^z \int_a^y x dx dy dz dt \right) f^{(4)}(\xi) g'(\eta) \quad (37)$$

Now, it is easy to obtain:

$$\begin{aligned}\int_a^\beta t \, dt &= \frac{\beta^2 - \alpha^2}{2} \\ \int_a^\beta \int_a^t x \, dx \, dt &= \frac{\beta^3}{6} - \frac{\alpha^2 \beta}{2} + \frac{\alpha^3}{3} \\ \int_a^\beta \int_a^t \int_a^y x \, dx \, dy \, dt &= \frac{\beta^4}{24} - \frac{\alpha^2 \beta^2}{4} + \frac{\alpha^3 \beta}{3} - \frac{\alpha^4}{8}.\end{aligned}$$

and, using these in (37), we finally get:

$$\int_a^\beta f(t) \, dt = \frac{\beta - \alpha}{2} [f(\alpha) + f(\beta)] - \frac{(\beta - \alpha)^3}{12} f''\left(\frac{\alpha + \beta}{2}\right) - \frac{(\beta - \alpha)^5}{480} f^{(4)}(\xi), \quad (38)$$

where which show the reducibility of proposed AMT quadrature its simple counterpart (10) [4]. It is a fact that the composite quadrature rules provides greater accuracy than the basic formulae. To reduce truncation error further from local to global application of AMT quadrature, the composite quadrature to (23) is referred here as AMCT, and with $\frac{b-a}{n} = h$ keeping the assumptions of Theorems 1-2 it can be written as:

$$\begin{aligned}\int_a^\beta f(t) \, dg &\approx AMCT = \left[\frac{n}{\beta - \alpha} \int_a^{x_1} g(t) \, dt - g(\alpha) \right] f(\alpha) \\ &+ \frac{n}{\beta - \alpha} \sum_{k=1}^{n-1} \left[\int_{x_k}^{x_{k+1}} g(t) \, dt - \int_{x_{k-1}}^{x_k} g(t) \, dx_i \right] f(x_k) \\ &+ \left[g(\beta) - \frac{n}{\beta - \alpha} \int_{x_{n-1}}^\beta g(t) \, dt \right] f(\beta) \\ &+ \sum_{i=1}^{n-1} \left[\int_{x_{k-1}}^{x_k} \int_{x_{k-1}}^t g(x) \, dx \, dt - \frac{h}{2} \int_{x_{k-1}}^k g(t) \, dt \right] f''\left(\frac{x_{k-1} + x_k}{2}\right) \quad (39)\end{aligned}$$

Theorem 4. Assuming continuity of $f(t)$ and $g(t)$ in $\frac{\beta - \alpha}{2}$ along with $g(t)$ being monotonically rising in the same interval. Suppose that $[\alpha, \beta]$ partitioned in n sub-intervals $[x_k, x_{k+1}]$ of size $h = \frac{\beta - \alpha}{n}$ in form of uniformly-spaced integration points: , for $k = 0, 1, \dots, n$. The AMCT quadrature with global truncation error $R_{AMCT}[f]$ is:

$$\begin{aligned}\int_a^\beta f(t) \, dg &= AMCT + R_{AMCT}[f] \\ &= \left[\frac{n}{\beta - \alpha} \int_a^{x_1} g(t) \, dt - g(\alpha) \right] f(\alpha) + \frac{n}{\beta - \alpha} \sum_{k=1}^{n-1} \left[\int_{x_k}^{x_{k+1}} g(t) \, dt - \int_{x_{k-1}}^{x_k} g(t) \, dx_i \right] f(x_k) \\ &\quad + \left[g(\beta) - \frac{n}{\beta - \alpha} \int_{x_{n-1}}^\beta g(t) \, dt \right] f(\beta)\end{aligned}$$

$$\begin{aligned}
& + \sum_{k=1}^{n-1} \left[\int_{x_{k-1}}^{x_k} \int_{x_{k-1}}^{x_t} g(x) dx dt - \frac{h}{2} \int_{x_{k-1}}^{x_k} g(t) dt \right] f'' \left(\frac{x_{i+1} + x_i}{2} \right) \\
& + n \left[\frac{2\alpha^3 + 2\alpha\beta^2 + 2\alpha^2\beta - 6\beta^3 + 3(\beta - \alpha)(\alpha + \beta)^2}{48} \int_a^\beta g(t) dt \right. \\
& \quad + \frac{4\beta^2 - (\alpha + \beta)^2}{8} \int_a^\beta \int_a^t g(x) dx dt \\
& \quad \left. - \beta \int_a^\beta \int_a^t \int_a^y g(x) dx dy dt + \int_a^\beta \int_a^t \int_a^y \int_a^z g(x) dx dy dz dt \right] f^{(4)}(\xi) g'(\eta) \quad (40)
\end{aligned}$$

where $\xi, \eta \in (\alpha, \beta)$

Proof. Refereeing to a local truncation error from (24) for the AMT quadrature, we have:

$$\begin{aligned}
& \left[\frac{2x_{p-1}^3 + 2x_{p-1}x_p^2 + 2x_{p-1}^2x_p - 6x_p^3 + 3(x_p - x_{p-1})(x_{p-1} + x_p)^2}{48} \int_{x_{p-1}}^{x_p} g(t) dt \right. \\
& + \frac{4x_p^2 - (x_{p-1} + x_p)^2}{8} \int_{x_{p-1}}^{x_p} \int_{x_{p-1}}^t g(x) dx dt - x_p \int_{x_{p-1}}^{x_p} \int_{x_{p-1}}^t \int_{x_{p-1}}^y g(x) dx dy dt \quad (41) \\
& \left. + \int_{x_{p-1}}^{x_p} \int_{x_{p-1}}^t \int_{x_{p-1}}^y \int_{x_{p-1}}^z g(x) dx dy dz dt \right] f^{(4)}(\xi_p) g'(\eta_p)
\end{aligned}$$

where $\xi_p, \eta \in (\alpha, \beta)$ Adding n such local truncation errors leads to the global truncation error as:

$$\begin{aligned}
& \sum_{k=1}^{n-1} \left[\frac{2x_{k-1}^3 + 2x_{k-1}x_k^2 + 2x_{k-1}^2x_k - 6x_k^3 + 3(x_k - x_{k-1})(x_{k-1} + x_k)^2}{48} \int_{x_{k-1}}^{x_k} g(t) dt \right. \\
& + \frac{4x_k^2 - (x_{k-1} + x_k)^2}{8} \int_{x_{k-1}}^{x_k} \int_{x_{k-1}}^t g(x) dx dt - x_k \int_{x_{k-1}}^{x_k} \int_{x_{k-1}}^t \int_{x_{k-1}}^y g(x) dx dy dt \\
& \left. + \int_{x_{k-1}}^{x_k} \int_{x_{k-1}}^t \int_{x_{k-1}}^y \int_{x_{k-1}}^z g(x) dx dy dz dt \right] f^{(4)}(\xi_k) g'(\eta) \quad (42)
\end{aligned}$$

$$\begin{aligned}
& = n \left(\frac{2\alpha^3 + 2\alpha\beta^2 + 2\alpha^2\beta - 6\beta^3 + 3(\beta - \alpha)(\alpha + \beta)^2}{48} \int_a^\beta g(t) dt \right. \\
& + \frac{4\beta^2 - (\alpha + \beta)^2}{8} \int_a^\beta \int_a^\beta g(x) dx dt - \beta \int_a^\beta \int_a^t \int_a^y g(x) dx dy dt \quad (43) \\
& \left. + \int_a^\beta \int_a^t \int_a^y \int_a^z g(x) dx dy dz dt \right) \left[\frac{1}{n} \sum_{k=1}^n f^{(4)}(\xi_k) g'(\eta) \right]
\end{aligned}$$

Let $M = \left[\frac{1}{n} \sum_{k=1}^n f^{(4)}(\xi_k) g'(\eta) \right]$

Clearly, $\min_{x \in [\alpha, \beta]} \{f^{(4)}(x)g^{(4)}(x)\} \leq M \leq \max_{x \in [\alpha, \beta]} \{f^{(4)}(x)g^{(4)}(x)\}$. Because $f^{(4)}(x)$ and $g'(x)$ in $[\alpha, \beta]$ are continuous, so there is a point μ such that $M = f^{(4)}(\mu)g'(\eta)$.

Finally, the global truncation error $R_{AMCT}[f]$ takes the form:

$$= n \left(\frac{2\alpha^3 + 2\alpha\beta^2 + 2\alpha^2\beta - 6\beta^3 + 3(\beta - \alpha)(\alpha + \beta)^2}{48} \int_a^\beta g(t) dt + \frac{4\beta^2 - (\alpha + \beta)^2}{8} \int_a^\beta \int_a^\beta g(x) dx dt \right. \\ \left. - \beta \int_a^\beta \int_a^t \int_a^y g(x) dx dy dt + \int_a^\beta \int_a^t \int_a^y \int_a^z g(x) dx dy dz dt \right) f^{(4)}(\mu)g'(\eta) \quad (44)$$

where $\mu, \eta \in (\alpha, \beta)$ and $h = \frac{\beta - \alpha}{n}$

2.2.2. Proposed derivative-based rules for the Riemann-Stieltjes integral using other means

Some other schemes are derived in terms of geometric, harmonic, heronian and centroidal means for RS-integral using the approach discussed in section 2.2.1. The derivation of the quadrature scheme, its error term and the consequent reduction to the classical Riemann integral case are in a same pattern as proved in Theorems 1-4, respectively. For brevity, we discuss the main results in form of corollaries here that have similar proofs to Theorems 1-4, and can also be considered immediate consequences of the process followed therein. In scheme (17), selecting the expression of c as the geometric, harmonic, heronian and centroidal means of the limits of integration, then the corresponding new trapezoid-type schemes for the RS integrals, labeled as: GMT, HaMT, HeMT and CMT, respectively, are described in Corollaries 1-4 with error terms in basic form.

Corollary 1. Assuming continuity of $f(t)$ and $g(t)$ in $[\alpha, \beta]$ along with $g(t)$ being monotonically rising in the same interval, GMT quadrature for the RS-integral is:

$$\int_a^\beta f(x) dg \approx GMT = \left(\frac{1}{\beta - \alpha} \int_a^\beta g(t) dt - g(\alpha) \right) f(\alpha) + \left(g(\beta) - \frac{1}{\beta - \alpha} \int_a^\beta g(t) dt \right) f(\beta) \\ + \left(\int_a^\beta \int_a^t g(x) dx dt - \frac{\beta - \alpha}{2} \int_a^\beta g(t) dt \right) f''(\sqrt{\alpha\beta}) \quad (45)$$

with precision 2. The error term $R_{GMT}[f]$ is:

$$\left(\frac{\alpha^2 + \alpha\beta - 2\beta^2 + 3\sqrt{\alpha\beta}(\beta - \alpha)}{6} \int_\alpha^\beta g(t) dt + (\beta - \sqrt{\alpha\beta}) \int_\alpha^\beta \int_\alpha^t g(x) dx dt \right. \\ \left. - \int_\alpha^\beta \int_\alpha^t \int_\alpha^y g(x) dx dy dt \right) f^{(3)}(\xi),$$

where $\xi \in (\alpha, \beta)$

Corollary 2. Assuming continuity of $f(t)$ and $g(t)$ in $[\alpha, \beta]$ along with $g(t)$ being monotonically rising in the same interval, HaMT quadrature for the RS-integral is:

$$\int_a^\beta f(x) dg \approx \text{HaMT} = \left(\frac{1}{\beta - \alpha} \int_a^\beta g(t) dt - g(\alpha) \right) f(\alpha) + \left(g(\beta) - \frac{1}{\beta - \alpha} \int_a^\beta g(t) dt \right) f(\beta) \\ + \left(\int_a^\beta \int_a^t g(x) dx dt - \frac{\beta - \alpha}{2} \int_a^\beta g(t) dt \right) f''\left(\frac{2\alpha\beta}{\alpha + \beta}\right) \quad (46)$$

with precision 2. The truncation error $R_{\text{HaMT}}[f]$ is:

$$\left(\frac{\alpha^3 - 4\alpha^2\beta + 5\alpha\beta^2 - 2\beta^3}{6(\alpha + \beta)} \int_\alpha^\beta g(t) dt + \left(\frac{\beta^2 - \alpha\beta}{\alpha + \beta} \right) \int_\alpha^\beta \int_\alpha^t g(x) dx dt \right. \\ \left. - \int_\alpha^\beta \int_\alpha^t \int_\alpha^y g(x) dx dy dt \right) f^{(4)}(\xi), \quad (47)$$

where $\xi \in (\alpha, \beta)$

Corollary 3. Assuming continuity of $f(t)$ and $g(t)$ in $[\alpha, \beta]$ along with $g(t)$ being monotonically rising in the same interval, HeMT quadrature for the RS-integral is:

$$\int_a^\beta f(x) dg \approx \text{HeMT} = \left(\frac{1}{\beta - \alpha} \int_a^\beta g(t) dt - g(\alpha) \right) f(\alpha) + \left(g(\beta) - \frac{1}{\beta - \alpha} \int_a^\beta g(t) dt \right) f(\beta) \\ + \left(\int_a^\beta \int_a^t g(x) dx dt - \frac{\beta - \alpha}{2} \int_a^\beta g(t) dt \right) f''\left(\frac{\alpha + \sqrt{\alpha\beta} + \beta}{3}\right) \quad (48)$$

with precision 2. The error term $R_{\text{HeMT}}[f]$ is

$$\left(\frac{(\beta - \alpha)(\sqrt{\alpha\beta} - \beta)}{6} \int_a^\beta g(t) dt + \frac{2\beta - \alpha - \sqrt{\alpha\beta}}{3} \int_a^\beta \int_a^t g(x) dx dt \right. \\ \left. - \int_a^\beta \int_a^t \int_a^y g(x) dx dy dt \right) f^{(3)}(\xi), \quad (49)$$

where $\xi \in (\alpha, \beta)$

Corollary 4. Assuming continuity of $f(t)$ and $g(t)$ in $[\alpha, \beta]$ along with $g(t)$ being monotonically rising in the same interval, CMT quadrature for the RS-integral is:

$$\int_a^\beta f(x) dg \approx \text{CMT} = \left(\frac{1}{\beta - \alpha} \int_a^\beta g(t) dt - g(\alpha) \right) f(\alpha) + \left(g(\beta) - \frac{1}{\beta - \alpha} \int_a^\beta g(t) dt \right) f(\beta) \\ + \left(\int_a^\beta \int_a^t g(x) dx dt - \frac{\beta - \alpha}{2} \int_a^\beta g(t) dt \right) f''\left(\frac{2(\alpha^2 + \alpha\beta + \beta^2)}{3(\alpha + \beta)}\right) \quad (50)$$

with precision 2. The error term $R_{CMT}[f]$ is:

$$\begin{aligned} & \left(\frac{2\alpha^2\beta - \alpha\beta^2 - \alpha^3}{6(\alpha + \beta)} \int_{\alpha}^{\beta} g(t) dt + \frac{\alpha\beta + \beta^2 - 2\alpha^2}{3(\alpha + \beta)} \int_{\alpha}^{\beta} \int_{\alpha}^t g(x) dx dt \right. \\ & \quad \left. - \int_{\alpha}^{\beta} \int_{\alpha}^t \int_{\alpha}^y g(x) dx dy dt \right) f^{(3)}(\xi), \end{aligned} \quad (51)$$

where $\xi \in (\alpha, \beta)$

It is trivial to verify the reduction of the GMT, HaMT, HeMT and CMT rules for the RS integral to the classical Riemann integral by choosing $g(t) = t$ in context of the proof of Theorem 3 for the AMT rule. Using $g(t) = t$ in (44), (46), (48) and (50) along with in the error terms (1), (47), (49) and (51), we obtain the corresponding schemes (11)-(14) for the Riemann integral [7]. The successful reducibility of proposed derivative-based rules to the counterparts for Riemann integral show that the proposed rules defined in Theorems 1-5 and Corollaries 1-4 are a sensible modification to the existing rules, the classical Trapezoid and Zhao et al. [5] rules. To guarantee higher accuracy and lower errors, the global/composite quadrature through (44), (46), (48) and (50) are referred as GMCT, HaMCT, HeMCT and CMCT, and are presented in Corollary 5.

Corollary 5. Assuming continuity of $f(t)$ and $g(t)$ in $[\alpha, \beta]$ along with $g(t)$ being monotonically rising in the same interval, and with, the composite form of the proposed schemes (45), (46), (48) and (50) are given in (52)-(55).

$$\begin{aligned} \int_a^{\beta} f(t) dg & \approx GMCT = \left[\frac{n}{\beta - \alpha} \int_a^{x_1} g(t) dt - g(\alpha) \right] f(\alpha) \\ & + \frac{n}{\beta - \alpha} \sum_{k=1}^{n-1} \left[\int_{x_k}^{x_{k+1}} g(t) dt - \int_{x_{k-1}}^{x_k} g(t) dt \right] f(x_k) + \left[g(\beta) - \frac{n}{\beta - \alpha} \int_{x_{n-1}}^{\beta} g(t) dt \right] f(\beta) \\ & + \sum_{k=1}^n \left[\int_{x_{k-1}}^{x_k} \int_{x_{k-1}}^t g(x) dx dt - \frac{h}{2} \int_{x_{k-1}}^{x_k} g(t) dt \right] f''(\sqrt{x_k x_{k-1}}) \end{aligned} \quad (52)$$

$$\begin{aligned} \int_a^{\beta} f(t) dg & \approx HaMCT = \left[\frac{n}{\beta - \alpha} \int_a^{x_1} g(t) dt - g(\alpha) \right] f(\alpha) \\ & + \frac{n}{\beta - \alpha} \sum_{k=1}^{n-1} \left[\int_{x_k}^{x_{k+1}} g(t) dt - \int_{x_{k-1}}^{x_k} g(t) dt \right] f(x_k) + \left[g(\beta) - \frac{n}{\beta - \alpha} \int_{x_{n-1}}^{\beta} g(t) dt \right] f(\beta) \\ & + \sum_{k=1}^n \left[\int_{x_{k-1}}^{x_k} \int_{x_{k-1}}^t g(x) dx dt - \frac{h}{2} \int_{x_{k-1}}^{x_k} g(t) dt \right] f''\left(\frac{2x_k x_{k-1}}{x_{k-1} + x_k}\right) \end{aligned} \quad (53)$$

$$\begin{aligned}
\int_a^\beta f(t) dg \approx HeMCT &= \left[\frac{n}{\beta - \alpha} \int_a^{x_1} g(t) dt - g(\alpha) \right] f(\alpha) \\
&+ \frac{n}{\beta - \alpha} \sum_{i=k}^{n-1} \left[\int_{x_k}^{x_{k+1}} g(t) dt - \int_{x_{k-1}}^{x_k} g(t) dt \right] f(x_k) + \left[g(\beta) - \frac{n}{\beta - \alpha} \int_{x_{n-1}}^\beta g(t) dt \right] f(\beta) \\
&+ \sum_{k=1}^n \left[\int_{x_{k-1}}^{x_k} \int_{x_{k-1}}^t g(x) dx dt - \frac{h}{2} \int_{x_{k-1}}^{x_i} g(t) dt \right] f'' \left(\frac{x_{k-1} + \sqrt{x_{k-1}x_i} + x_k}{3} \right)
\end{aligned} \tag{54}$$

$$\begin{aligned}
\int_a^\beta f(t) dg \approx CMCT &= \left[\frac{n}{\beta - \alpha} \int_a^{x_1} g(t) dt - g(\alpha) \right] f(\alpha) \\
&+ \frac{n}{\beta - \alpha} \sum_{k=1}^{n-1} \left[\int_{x_k}^{x_{k+1}} g(t) dt - \int_{x_{k-1}}^{x_k} g(t) dt \right] f(x_k) \\
&+ \left[g(\beta) - \frac{n}{\beta - \alpha} \int_{x_{n-1}}^\beta g(t) dt \right] f(\beta) \\
&+ \sum_{k=1}^n \left[\int_{x_{k-1}}^{x_k} \int_{x_{k-1}}^t g(x) dx dt - \frac{h}{2} \int_{x_{k-1}}^{x_i} g(t) dt \right] f'' \left(\frac{2(x_{k-1}^2 + x_{k-1}x_k + x_k^2)}{3(x_{k-1} + x_k)} \right)
\end{aligned} \tag{55}$$

Unlike the standard form of the truncation error (43) of the proposed AMCT quadrature, the same cannot be expected for the case of proposed trapezoid-type quadrature with other averages. This is because of the non-conventional expressions of type $(\sqrt{b}) - \sqrt{a})$, $(\alpha + \beta)$, etc. in local truncation errors in addition to the usual conventional exponents of $(\beta - \alpha)$; as also obvious from the definition 3.

However, the ZCT [5] quadrature's composite form, though not presented in [5], takes the form:

$$\begin{aligned}
\int_a^\beta f(t) dg \approx ZCT &= \left[\frac{n}{\beta - \alpha} \int_a^{x_1} g(t) dt - g(\alpha) \right] f(\alpha) \\
&+ \frac{n}{\beta - \alpha} \sum_{k=1}^{n-1} \left[\int_{x_k}^{x_{k+1}} g(t) dt - \int_{x_{k-1}}^{x_k} g(t) dt \right] f(x_k) \\
&+ \left[g(\beta) - \frac{n}{\beta - \alpha} \int_{x_{n-1}}^\beta g(t) dt \right] f(\beta) \\
&+ \sum_{k=1}^n \left[\int_{x_{k-1}}^{x_k} \int_{x_{k-1}}^t g(x) dx dt - \frac{h}{2} \int_{x_{k-1}}^{x_k} g(t) dt \right] g(t) f''(\varepsilon_k)
\end{aligned} \tag{56}$$

$$\begin{aligned}
n \left(\frac{\alpha^3 + \alpha\beta^2 + \alpha^2\beta - 3\beta^3 + 6(\beta - \alpha)c^2}{24} \int_\alpha^\beta g(t) dt + \frac{\beta^2 - c^2}{2} \int_\alpha^\beta \int_\alpha^t g(x) dx dt \right. \\
\left. - \beta \int_\alpha^\beta \int_\alpha^t \int_\alpha^y g(x) dx dy dt + \int_\alpha^\beta \int_\alpha^t \int_\alpha^y \int_\alpha^z g(x) dx dy dz dt \right) f^{(4)}(\xi) g'(\eta)
\end{aligned} \tag{57}$$

where $\mu, \eta \in [\alpha, \beta]$. Now, we describe the composite form MZCT of MZT [22] in (57).

$$\begin{aligned}
\int_a^\beta f(t) dg \approx MZCT &= \left[\frac{n}{\beta - \alpha} \int_a^{x_1} g(t) dt - g(\alpha) \right] f(\alpha) \\
&+ \frac{n}{\beta - \alpha} \sum_{k=1}^{n-1} \left[\int_{x_k}^{x_{k+1}} g(t) dt - \int_{x_{k-1}}^{x_k} g(t) dt \right] f(x_i) \\
&+ \left[g(\beta) - \frac{n}{\beta - \alpha} \int_{x_{n-1}}^\beta g(t) dt \right] f(\beta) \\
&+ \sum_{k=1}^n \left[\int_{x_{k-1}}^{x_k} \int_{x_{k-1}}^t g(x) dx dt - \frac{h}{2} \int_{x_{k-1}}^{x_k} g(t) dt \right] g(t) f''(\varepsilon_i)
\end{aligned} \tag{58}$$

$$\begin{aligned}
& n \left(\frac{\alpha^3 + \alpha\beta^2 + \alpha^2\beta - 3\beta^3 + 6(\beta - \alpha)c^2}{24} \int_{\alpha}^{\beta} g(t) dt + \frac{\beta^2 - c^2}{2} \int_{\alpha}^{\beta} \int_{\alpha}^t g(x) dx dt \right. \\
& \quad \left. - \beta \int_{\alpha}^{\beta} \int_{\alpha}^t \int_{\alpha}^y g(x) dx dy dt + \int_{\alpha}^{\beta} \int_{\alpha}^t \int_{\alpha}^y \int_{\alpha}^z g(x) dx dy dz dt \right) f^{(4)}(\xi) g'(\eta)
\end{aligned} \tag{59}$$

where $\mu, \eta \in (\alpha, \beta)$.

3. Results of the numerical experiments and their discussion

We examine the performance of the proposed quadrature of Trapezoid-type for RS-integral over original Trapezoid, Zhao et al. [5] and modified Zhao-Trapezoid (MZT) [22] rules in terms of absolute error distributions when integration strips are increased. In addition, we also compute computational/observed order of accuracy/exactness of proposed quadrature so that the theoretical expressions in Theorems 1-4 and Corollaries 1-5 are verified. It should be noted that in the previous studies [3], [5], the numerical experiments were not performed on the quadrature schemes for the RS-integral ; however, this research verifies the theoretical results by experimental results solving five different examples. Five problems are taken from [21], [23],[24], [13] and [14], and these are tested in approximations up to 16 decimal places of accuracy using the MATLAB software. The results were noted using the Intel (R) Core (TM) Laptop using 4GB RAM operating at speed of 0.80 GHz – 1.00 GHz. Also, the double precision default arithmetic of MATLAB is utilized for the results.

(i) Example 1 $\int_{4.5}^{3.5} \sin 5x d(\cos x) = 0.227676016130689$

(ii) Example 2 $\int_5^6 \sin x d(x^3) = 59.655908136641912$

(iii) Example 3 $\int_5^6 e^x d(\sin x) = 187.4269314248657$

(iv) Example 4 $\int_0^{pi} x^3 d(\sin x) = -17.608813203268074$

(v) Example 5 $\int_{-1}^1 x^3 d(e^x) = -17.608813203268074$

The formula of absolute error drop (AED) [9] is:

$$AED = |EVAV| \tag{60}$$

In (60), AE and AV refer to exact and approximate values of integrals, respectively. The formula for the observed/computational order of accuracy is defined in [25], [24], [13], [14] as:

$$p = \frac{\ln \left(\frac{|N(2h) - N(0)|}{|N(h) - N(0)|} \right)}{\ln 2}. \quad (61)$$

where N indicates approximate quadrature result at the step-size indicated in the parenthesis, and with 0 inside the base result – the exact integral value – is intended.

Figs. (3)-(7), respectively, display AEDs for the case of examples 1-5 for the quadrature approximations of previous quadrature: Trapezoid CT [20], ZCT [5] and MZCT [22], and the new trapezoid-type quadrature: AMCT, GMCT, HMCT, HeMCT and CMCT. For numerical test integrals 1-3 through Figs.(3)-(5), it is obvious to note the ascending performance of the proposed quadrature. The AEDs for the CMCT quadrature are lowest of all for test numerical integrals 1-3, and the AEDs in the case of existing quadrature CT and ZCT are much slower (3)-(5). The ZCT quadrature [5] is less likely to assure the claimed units of precision and accuracy as in [5], but MZCT quadrature [22] exhibits obvious improvement over the ZCT quadrature in all test integrals. The ZCT quadrature behaves poorest of all in the case of problems 4-5. In problems 4-5 (see Figs. (6)-(7)), the new quadrature proposed in this study result in smaller AEDs when compared with ZCT and CT quadrature. Also, the MZCT quadrature [22] assures smallest AED than what was expected in single strip, but then the AEDs do not get smaller rapidly since we used double precision default in MATLAB. To avoid the disturbance in results due to ZCT oscillations in decreasing errors, the AEDs for examples 1-5 are also displayed in Figs. (8)-(12) without the ZCT errors. The Figs. (8)-(12) provide more comprehensive and clearer picture of the performance of the new proposed rules with each other and the CT in terms of decreasing AEDs. Table (1) summarizes quadrature results for problems 1-5 and corresponding AEDs at the final integration strip, which evidently confirms that the proposed quadrature assures smaller AEDs against ZCT and CT in all problems taken; the CMCT quadrature being the best in problems 1-3. The results of MZCT quadrature [22] are pretty inclined near the proposed quadrature for problems 1-3, but the default double precision limit in problems 4-5 restricts MZCT quadrature to rapidly reduce errors ahead. Hence, the proposed quadrature exhibit stable pattern of AEDs.

In tables (2)-(6), we present the computational/observed results on the orders of exactness/accuracy for all used quadrature for the case of problems 1-5 through the methodology described in [22]. For the case of ZCT quadrature with reference to the tables (2)-(4), the numerical results on order of exactness are not in line with what was expected through [5]. However, the MZCT and all the proposed quadrature results tend to the expected theoretical results. The MZCT quadrature results on numerical order of accuracy cannot be actualized because of precision limits in the case of problems 4-5; ACT quadrature also did not result in expected accuracy in [5]. On the other hand, all the proposed quadrature actualize the theoretically expected results in terms of the numerical results presented in Tables (2)-(6), with the only exception of the two: GMCT and HeMCT for the problem 5 alone through Table 6. The exception is result of the fact that these two rules have

limitation for the limits of integration being different signs; this was the case in problem 5. Similarly, there is an exception for the two quadrature formulae: HMCT and CMCT for the problem 5 as zero denominators are caused since limits add to zero, but only for odd strips. Both the rules are applicable safely in the alternate cases with even strips. We highlight that the selection of numerical problems in this study was done in the form of problems 1-5 intentionally from the literature so that the best coverage of use, restrictions and performance of all the quadrature used can be done sufficiently. The quadrature formulae in the case compared previous and new rules differ in the fact that these utilize different information of integrand and integrator functions, their derivatives and integrations. Hence, it is mandatory to observe the computational overhead/cost through the information content used in the formulae and also discuss the CPU usage time (in seconds) when all the quadrature formulae are applied to solve problems 1-5 under similar conditions to achieve a given error bound. Table (7) presents the distribution of evaluations in the formulae of all used quadrature. Tables (8)-(12) summarize distribution of computational cost for all used quadrature when the preset error tolerance was kept at 10^{-5} for problems 1-5. Also, the net computational costs for problems 1-5 are displayed in Tables (8)-(12). The results in Tables (8)-(12) and corresponding last columns in these highlight the cost effectiveness of the proposed quadrature formulae over ZCT, CT and MZCT in all problems, but with exception for for GMCT and HeMCT quadrature for problem 5 only. From Tables (11)-(12) in the case of problems 4-5, it is again reconfirmed that the ZCT quadrature is not applicable; the MZCT quadrature restrict to first strip of integration only and all the new quadrature show better performance for the cost efficiency. In the same way to achieve a preset AED of at most 10^{-5} , the performance of all the used quadrature was tested with regards to the time efficiency, and these results are presented in Table (13) for all problems in form of execution times (in seconds). Table 13 highlights that the AMCT and CMCT quadrature exhibit smallest times mostly, except for problems 4-5 than MZCT quadrature, which is restricted to first strip only. Finally, it can be safely concluded that the proposed quadrature exhibit encouraging and better performance overall than the previous CT and ZCT quadrature.

Table 1: Absolute errors are compared to all schemes for Examples 1-5

| Trapezoid Variant | Example 1 ($n = 50$) | Example 2 ($n = 200$) | Example 3 ($n = 50$) | Example 4 ($n = 50$) | Example 5 ($n = 50$) |
|-------------------|--|---|--|---|--|
| CT | 0.227486276308570 (1.8974×10^{-4}) | -59.655783853372625 (1.2428×10^{-4}) | 187.4331788489458 (6.2474×10^{-3}) | -17.612760265633682 (3.9471×10^{-3}) | 0.450095792679060 (5.8839×10^{-4}) |
| ZCT | 0.227524664135771 (1.5135×10^{-4}) | -59.655762104211938 (1.4603×10^{-4}) | 187.4331788489458 (6.2474×10^{-3}) | -29.345389591343285 ($1.1737 \times 10^{+1}$) | -1.30536248.6941216 ($1.7549 \times 10^{+0}$) |
| MZCT | 0.227676063572853 (4.7442×10^{-8}) | -59.655908136719574 (7.7648×10^{-11}) | 1.874269314873392 (6.2473×10^{-8}) | -17.608813203268074 (1.9201×10^{-15}) | 0.449507401824980 (-7.1054×10^{-15}) |
| AMCT | 0.227676057801290 (4.1671×10^{-8}) | -59.655908136739335 (9.7423×10^{-11}) | 187.4269315224149 (9.7549×10^{-8}) | -17.608813463050069 (2.5978×10^{-7}) | 0.449507451964994 (5.0140×10^{-8}) |
| GMCT | 0.227676058321505 (4.2191×10^{-8}) | -59.655908136813444 (1.7153×10^{-10}) | 187.4269315777802 (1.5291×10^{-7}) | -17.608807372830086 (5.8304×10^{-6}) | 0.449086933331309 (4.2047×10^{-4}) |
| HaMCT | 0.227676058841074 (4.2710×10^{-8}) | -59.655908136887568 (2.4566×10^{-10}) | 187.4269316331454 (2.0828×10^{-7}) | -17.608805228593440 (7.9747×10^{-6}) | 0.449508128616925 (7.2679×10^{-7}) |
| HeMCT | 0.227676057974770 (4.1844×10^{-8}) | -59.655908136764033 (1.2212×10^{-10}) | 187.4269315408704 (1.1600×10^{-7}) | -17.608811432976740 (1.7703×10^{-6}) | 0.449367279087097 (1.4012×10^{-4}) |
| CMCT | 0.227676057454114 (4.1323×10^{-8}) | -59.655908136689931 (4.8018×10^{-11}) | 187.4269314855043 (6.0639×10^{-8}) | -17.608816207868944 (3.0046×10^{-6}) | 0.449507226414350 (1.7541×10^{-7}) |

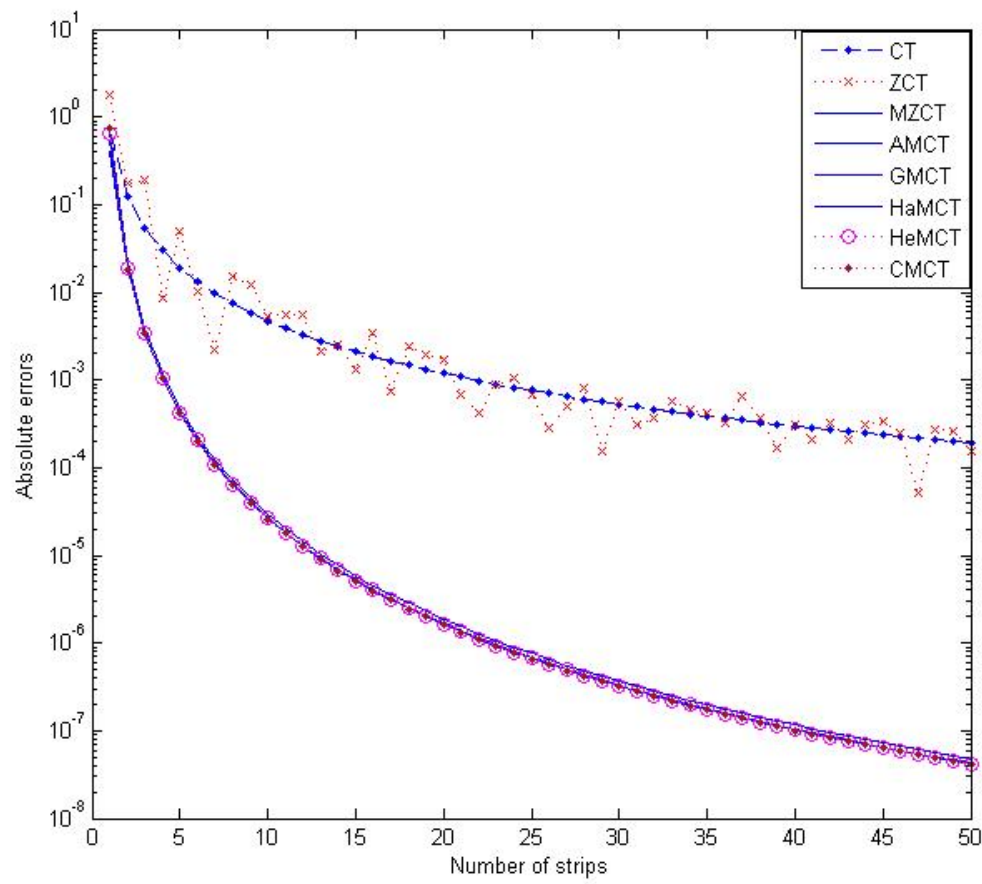


Figure 3: Distributions of absolute-error-drops in Example 1

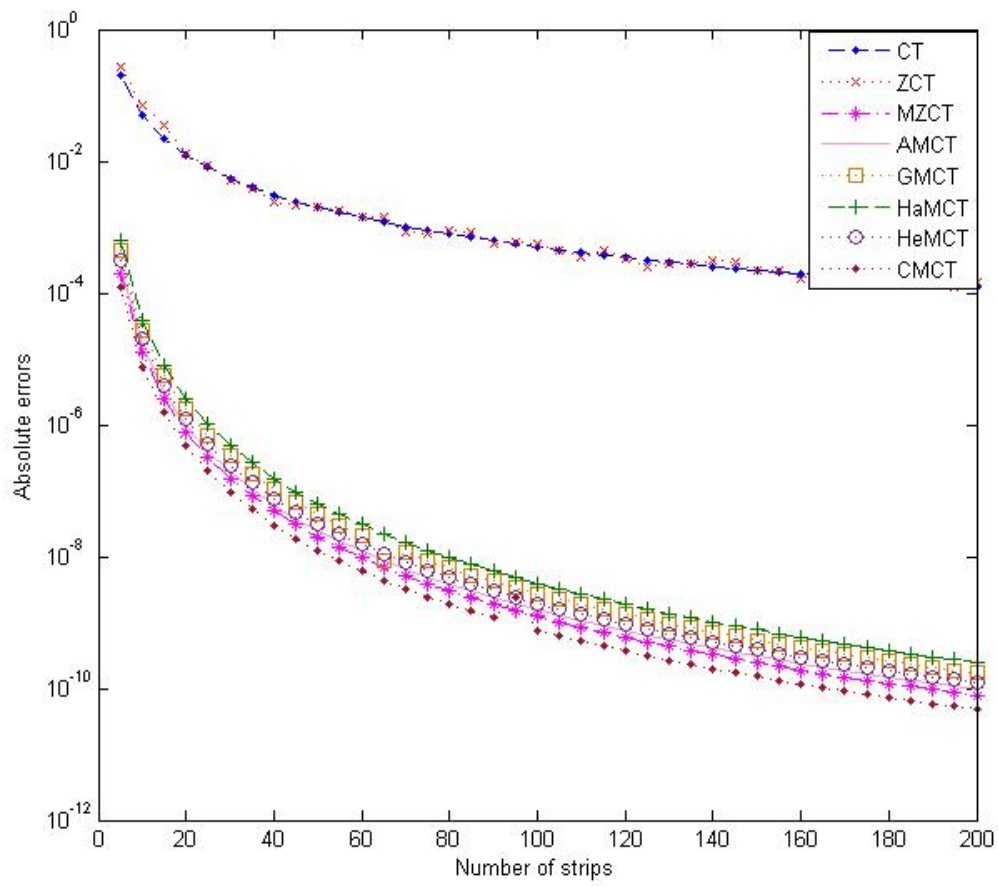


Figure 4: Distributions of absolute-error-drops in Example 2

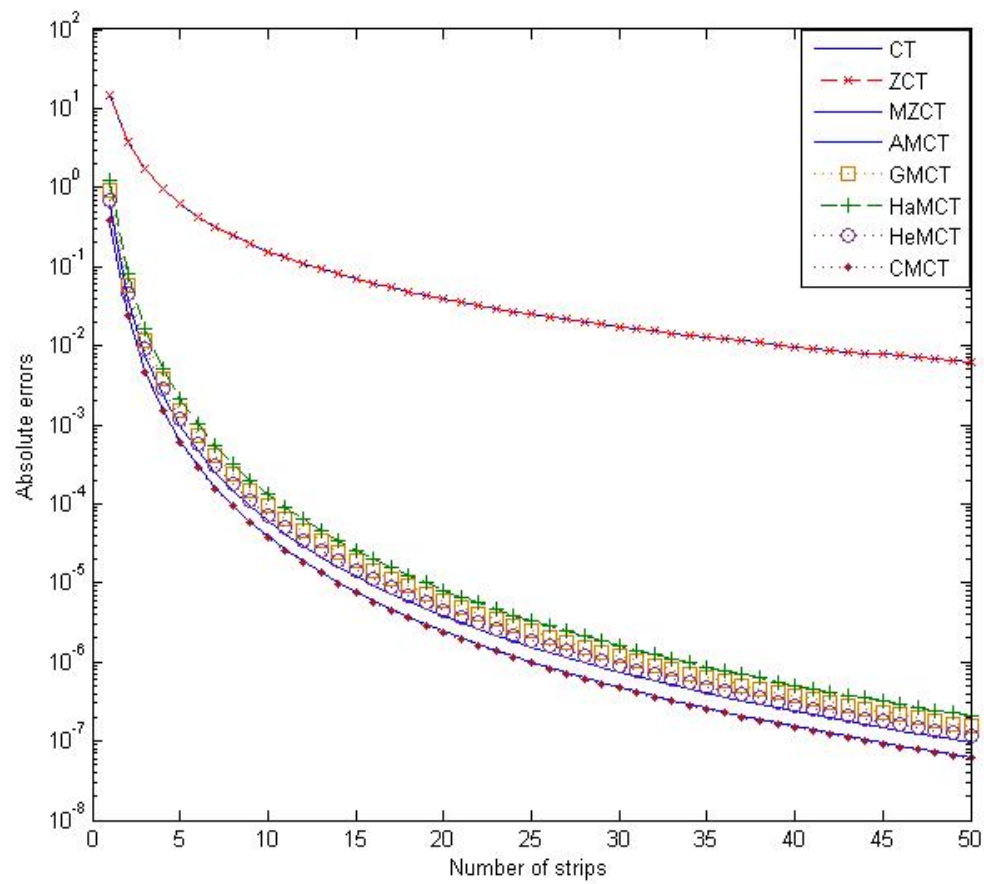


Figure 5: Distributions of absolute-error-drops in Example 3

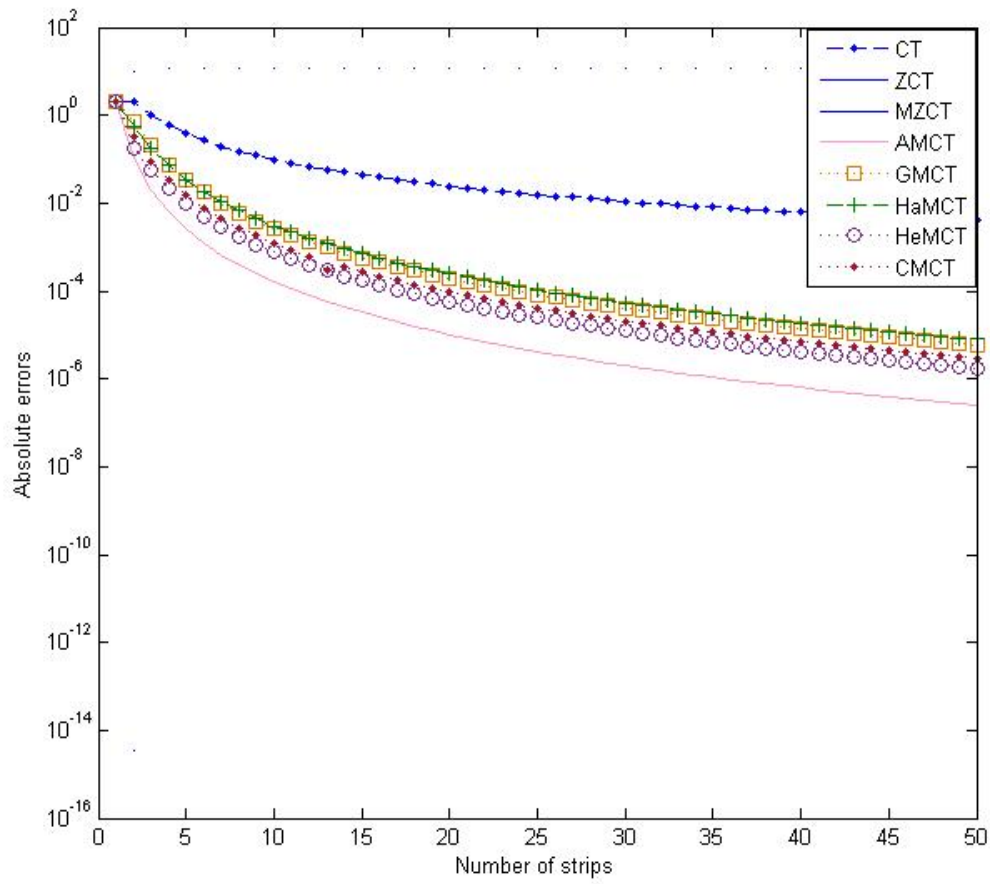


Figure 6: Distributions of absolute-error-drops in Example 4

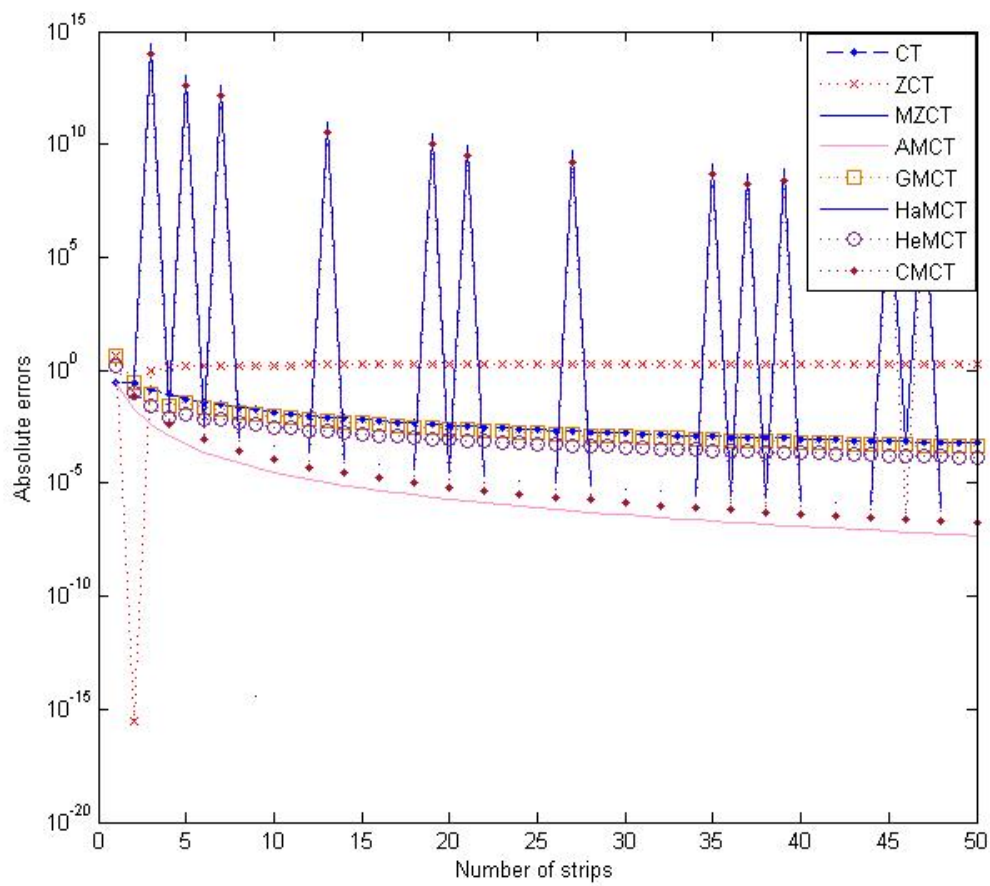
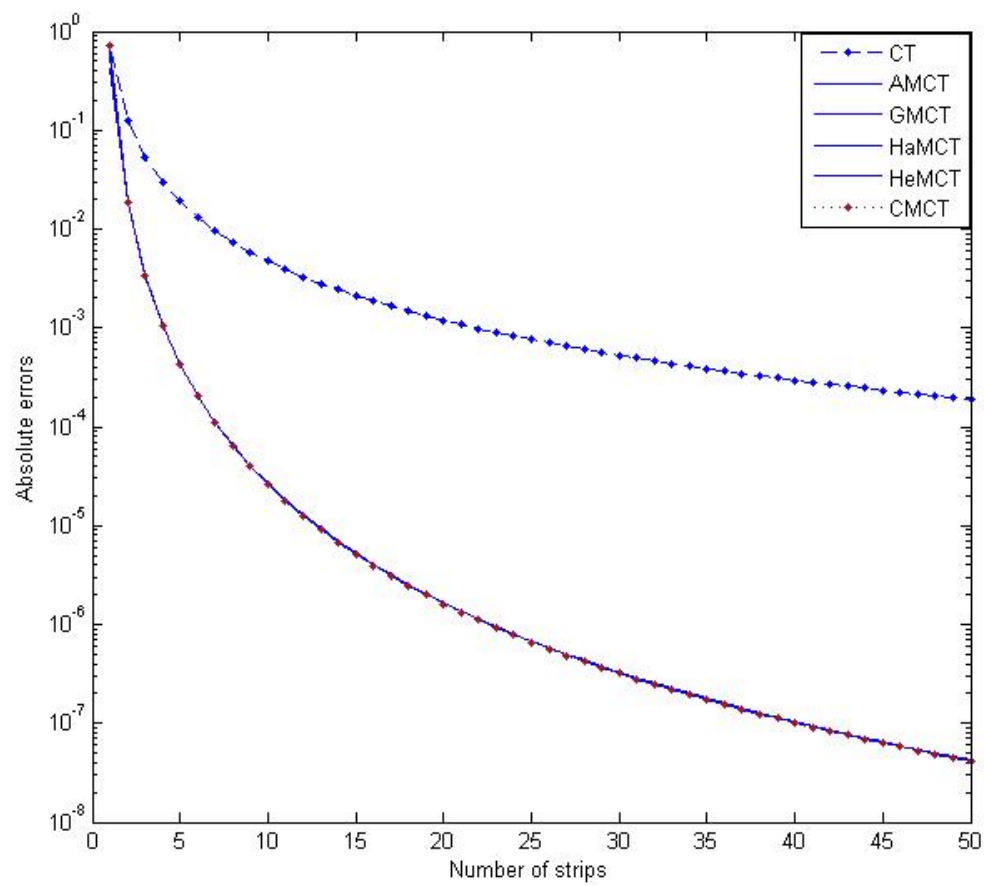


Figure 7: Distributions of absolute-error-drops in Example 5

Figure 8: Distributions of absolute-error-drops without ZCT in Example 1

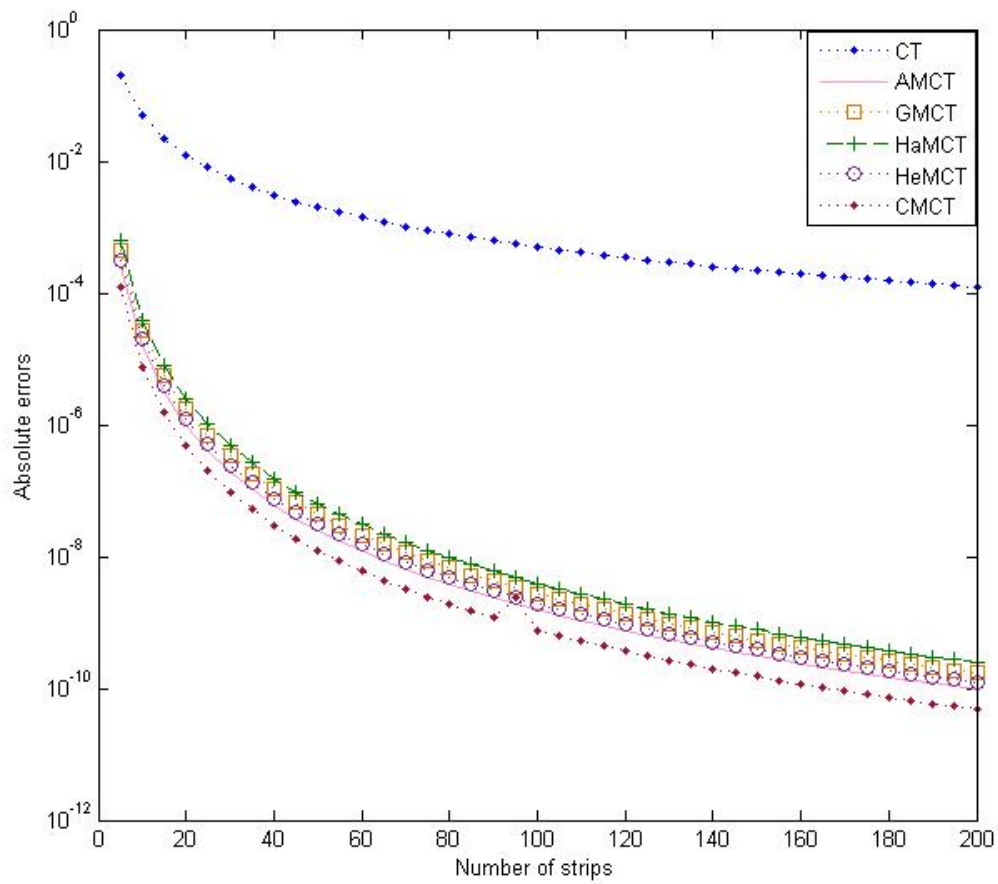


Figure 9: Distributions of absolute-error-drops without ZCT in Example 2

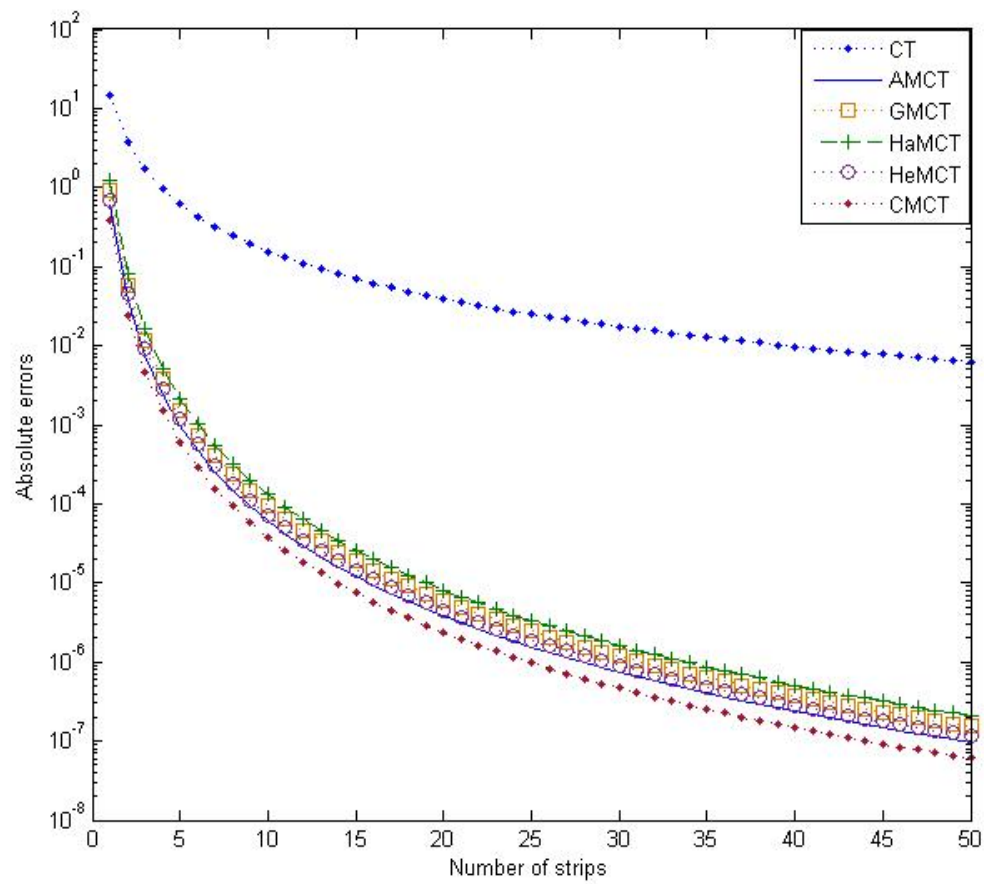


Figure 10: Distributions of absolute-error-drops without ZCT in Example 3

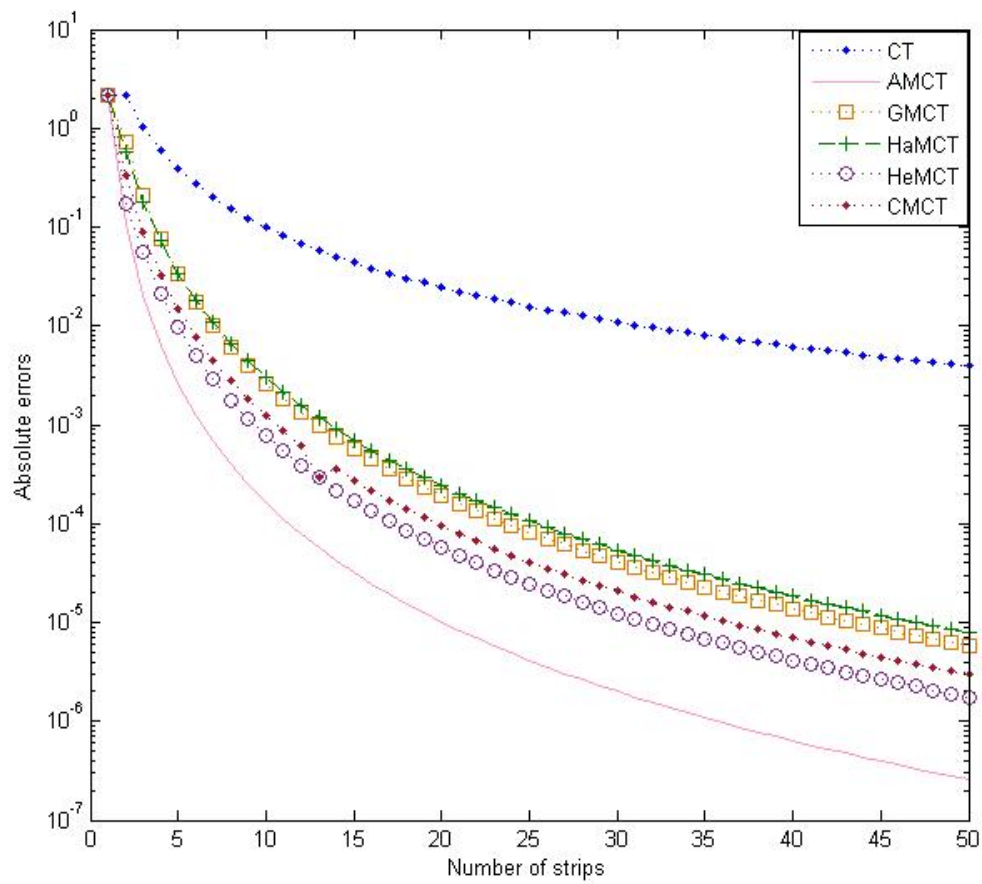


Figure 11: Distributions of absolute-error-drops without ZCT in Example 4

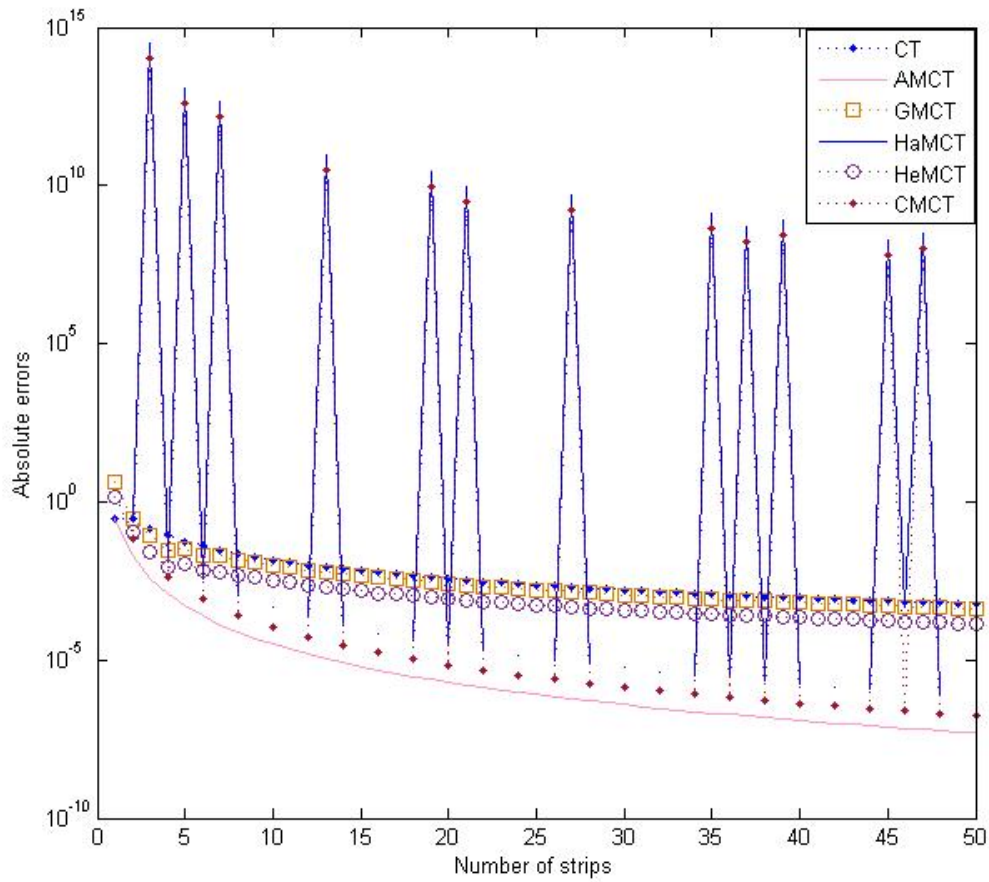


Figure 12: Distributions of absolute-error-drops without ZCT in Example 5

Table 2: . Representation of the order of accuracy to all schemes for Example 1

| m | n | CT | ZCT | MZCT | AMCT | GMCT | HaMCT | HeMCT | CMCT |
|-----|-----|--------|---------|--------|--------|--------|--------|--------|--------|
| 1 | 1 | NA | NA | NA | NA | NA | NA | NA | NA |
| 2 | 2 | 2.5728 | 3.3788 | 5.0724 | 5.1766 | 4.9006 | 4.4721 | 5.0970 | 5.3064 |
| 4 | 4 | 2.0420 | 4.3106 | 4.1474 | 4.1447 | 4.1338 | 4.1124 | 4.1422 | 4.1459 |
| 8 | 8 | 2.0091 | -0.8154 | 4.0348 | 4.0338 | 4.0317 | 4.0272 | 4.0334 | 4.0338 |
| 16 | 16 | 2.0022 | 2.1713 | 4.0086 | 4.0083 | 4.0078 | 4.0067 | 4.0082 | 4.0083 |
| 32 | 32 | 2.0006 | 3.2118 | 4.0021 | 4.0021 | 4.0020 | 4.0017 | 4.0021 | 4.0021 |
| 64 | 64 | 2.0001 | 1.1185 | 4.0006 | 4.0006 | 4.0005 | 4.0004 | 4.0005 | 4.0005 |

Table 3: Representation of the order of accuracy to all schemes for Example 2

| m | n | CT | ZCT | MZCT | AMCT | GMCT | HaMCT | HeMCT | CMCT |
|-----|-----|--------|--------|--------|--------|--------|--------|--------|--------|
| 5 | 5 | NA | NA | NA | NA | NA | NA | NA | NA |
| 10 | 10 | 2.0018 | 1.9243 | 4.0025 | 4.0022 | 4.0017 | 4.0010 | 4.0020 | 4.0030 |
| 20 | 20 | 2.0004 | 2.4487 | 4.0007 | 4.0006 | 4.0004 | 4.0003 | 4.0005 | 4.0008 |
| 40 | 40 | 2.0001 | 2.3985 | 4.0001 | 4.0002 | 4.0002 | 4.0000 | 4.0001 | 4.0002 |
| 80 | 80 | 2.0001 | 1.4026 | 4.0000 | 4.0000 | 4.0000 | 4.0001 | 4.0000 | 4.0001 |
| 160 | 160 | 2.0000 | 2.4557 | 3.9998 | 4.0001 | 4.0001 | 4.0001 | 4.0001 | 4.0002 |

Table 4: Representation of the order of accuracy to all schemes for Example 3

| m | n | CT | ZCT | MZCT | AMCT | GMCT | HaMCT | HeMCT | CMCT |
|-----|-----|--------|--------|--------|--------|--------|--------|--------|--------|
| 1 | 1 | NA | NA | NA | NA | NA | NA | NA | NA |
| 2 | 2 | 1.9319 | 1.9319 | 3.8984 | 3.9697 | 3.9467 | 3.9283 | 3.9610 | 3.9970 |
| 4 | 4 | 1.9844 | 1.9844 | 3.9761 | 3.9935 | 3.9878 | 3.9832 | 3.9913 | 4.0003 |
| 8 | 8 | 1.9962 | 1.9962 | 3.9941 | 3.9984 | 3.9971 | 3.9958 | 3.9979 | 4.0002 |
| 16 | 16 | 1.9990 | 1.9990 | 3.9985 | 3.9996 | 3.9992 | 3.9990 | 3.9995 | 4.0000 |
| 32 | 32 | 1.9998 | 1.9998 | 3.9996 | 3.9999 | 3.9998 | 3.9998 | 3.9999 | 4.0000 |
| 64 | 64 | 1.9999 | 1.9999 | 3.9999 | 4.0000 | 4.0000 | 3.9999 | 4.0000 | 4.0000 |

Table 5: Representation of the order of accuracy to all schemes for Example 4

| m | n | CT | ZCT | MZCT | AMCT | GMCT | HaMCT | HeMCT | CMCT |
|-----|-----|--------|---------|------|--------|--------|--------|--------|--------|
| 1 | 1 | NA | NA | NA | NA | NA | NA | NA | NA |
| 2 | 2 | 0 | NA | NA | 4.3044 | 1.5452 | 1.9113 | 3.6353 | 2.6795 |
| 4 | 4 | 1.8345 | 0.1972 | NA | 4.0662 | 3.2559 | 2.9653 | 3.0169 | 3.3438 |
| 8 | 8 | 1.9649 | 0.0404 | NA | 4.0160 | 3.6533 | 3.4400 | 3.5898 | 3.5701 |
| 16 | 16 | 1.9916 | 0.0095 | NA | 4.0040 | 3.7589 | 3.6076 | 3.7252 | 3.6758 |
| 32 | 32 | 1.9979 | 0.0025 | NA | 4.0010 | 3.8029 | 3.6944 | 3.7801 | 3.7374 |
| 64 | 64 | 1.9995 | 0.00061 | NA | 4.0002 | 3.8289 | 3.7487 | 3.8118 | 3.7784 |

Table 6: Representation of the order of accuracy to all schemes for Example 5

| m | n | CT | ZCT | MZCT | AMCT | GMCT | HaMCT | HeMCT | CMCT |
|-----|-----|--------|---------|--------|--------|--------|--------|--------|--------|
| 1 | 1 | NA | NA | NA | NA | NA | NA | NA | NA |
| 2 | 2 | 0 | 53.7424 | 1.0000 | 3.9032 | 3.9499 | NA | 3.7927 | NA |
| 4 | 4 | 1.7226 | 51.8971 | 1.0000 | 3.9747 | 3.3325 | 4.0089 | 3.6427 | 4.0217 |
| 8 | 8 | 1.9363 | 0.3302 | 1.5850 | 3.9936 | 1.0357 | 4.0023 | 0.9225 | 4.0055 |
| 16 | 16 | 1.9844 | 0.0725 | NA | 3.9984 | 1.8139 | 4.0005 | 1.8014 | 4.0014 |
| 32 | 32 | 1.9962 | 0.0176 | NA | 3.9996 | 1.9516 | 4.0001 | 1.9489 | 4.0003 |
| 64 | 64 | 1.9990 | 0.0044 | NA | 3.9999 | 1.9867 | 4.0000 | 1.9861 | 4.0001 |

Table 7: Total Computational cost in Trapezoidal variants for n sub-intervals

| Trapezoidal Variants | f | g | $f^{(1)}$ | $f^{(2)}$ | I_1 | I_2 | I_3 | Total evaluations | Total (n=1) |
|----------------------|-------|-----|-----------|-----------|-------|-------|-------|-------------------|-------------|
| CT | $n+1$ | 2 | 0 | 0 | n | 0 | 0 | $2n+3$ | 5 |
| ZCT | $n+1$ | 2 | 0 | n | n | n | n | $5n+3$ | 8 |
| MZCT | $n+1$ | 2 | 0 | n | n | n | n | $5n+3$ | 8 |
| AMCT | $n+1$ | 2 | 0 | n | n | n | 0 | $4n+3$ | 7 |
| GMCT | $n+1$ | 2 | 0 | n | n | n | 0 | $4n+3$ | 7 |
| HaMCT | $n+1$ | 2 | 0 | n | n | n | 0 | $4n+3$ | 7 |
| HeMCT | $n+1$ | 2 | 0 | n | n | n | 0 | $4n+3$ | 7 |
| CMCT | $n+1$ | 2 | 0 | n | n | n | 0 | $4n+3$ | 7 |

Table 8: Computational cost in Trapezoidal variants to achieve $\xi \leq 10^{-5}$ in Example 1

| Trapezoidal Variants | f | g | $f^{(1)}$ | $f^{(2)}$ | I_1 | I_2 | I_3 | Total evaluations |
|----------------------|-----|-----|-----------|-----------|-------|-------|-------|-------------------|
| CT | 219 | 2 | 0 | 0 | 218 | 0 | 0 | 439 |
| ZCT | 209 | 2 | 0 | 208 | 208 | 208 | 208 | 1043 |
| MZCT | 15 | 2 | 0 | 14 | 14 | 14 | 14 | 73 |
| AMCT | 14 | 2 | 0 | 13 | 13 | 13 | 0 | 55 |
| GMCT | 14 | 2 | 0 | 13 | 13 | 13 | 0 | 55 |
| HaMCT | 14 | 2 | 0 | 13 | 13 | 13 | 0 | 55 |
| HeMCT | 14 | 2 | 0 | 13 | 13 | 13 | 0 | 55 |
| CMCT | 14 | 2 | 0 | 13 | 13 | 13 | 0 | 55 |

Table 9: Computational cost in Trapezoidal variants to achieve $\xi \leq 10^{-5}$ in Example 2

| Trapezoidal Variants | f | g | $f^{(1)}$ | $f^{(2)}$ | I_1 | I_2 | I_3 | Total evaluations |
|----------------------|-----|-----|-----------|-----------|-------|-------|-------|-------------------|
| CT | 707 | 2 | 0 | 0 | 706 | 0 | 0 | 1415 |
| ZCT | 701 | 2 | 0 | 700 | 700 | 700 | 700 | 3503 |
| MZCT | 16 | 2 | 0 | 15 | 15 | 15 | 15 | 78 |
| AMCT | 13 | 2 | 0 | 12 | 12 | 12 | 0 | 51 |
| GMCT | 14 | 2 | 0 | 13 | 13 | 13 | 0 | 55 |
| HaMCT | 16 | 2 | 0 | 15 | 15 | 15 | 0 | 63 |
| HeMCT | 13 | 2 | 0 | 12 | 12 | 12 | 0 | 51 |
| CMCT | 11 | 2 | 0 | 10 | 10 | 10 | 0 | 43 |

Table 10: Computational cost in Trapezoidal variants to achieve $\xi \leq 10^{-5}$ accuracy in Example 3

| Trapezoidal Variants | f | g | $f^{(1)}$ | $f^{(2)}$ | I_1 | I_2 | I_3 | Total evaluations |
|----------------------|------|-----|-----------|-----------|-------|-------|-------|-------------------|
| CT | 1251 | 2 | 0 | 0 | 1250 | 0 | 0 | 2503 |
| ZCT | 1251 | 2 | 0 | 1250 | 1250 | 1250 | 1250 | 6253 |
| MZCT | 16 | 2 | 0 | 15 | 15 | 15 | 15 | 78 |
| AMCT | 17 | 2 | 0 | 16 | 16 | 16 | 0 | 67 |
| GMCT | 19 | 2 | 0 | 18 | 18 | 18 | 0 | 75 |
| HaMCT | 20 | 2 | 0 | 19 | 19 | 19 | 0 | 79 |
| HeMCT | 18 | 2 | 0 | 17 | 17 | 17 | 0 | 71 |
| CMCT | 15 | 2 | 0 | 14 | 14 | 14 | 0 | 59 |

Table 11: Computational cost in Trapezoidal variants to achieve $\xi \leq 10^{-5}$ accuracy in Example 4

| Trapezoidal Variants | f | g | $f^{(1)}$ | $f^{(2)}$ | I_1 | I_2 | I_3 | Total evaluations |
|----------------------|-----|-----|-----------|-----------|-------|-------|-------|-------------------|
| CT | 995 | 2 | 0 | 0 | 994 | 0 | 0 | 1991 |
| ZCT | — | — | — | — | — | — | — | — |
| MZCT | — | — | — | — | — | — | — | — |
| AMCT | 22 | 2 | 0 | 21 | 21 | 21 | 0 | 87 |
| GMCT | 45 | 2 | 0 | 44 | 44 | 44 | 0 | 179 |
| HaMCT | 49 | 2 | 0 | 48 | 48 | 48 | 0 | 195 |
| HeMCT | 33 | 2 | 0 | 32 | 32 | 32 | 0 | 131 |
| CMCT | 38 | 2 | 0 | 37 | 37 | 37 | 0 | 151 |

Table 12: Computational cost in Trapezoidal variants to achieve $\xi \leq 10^{-5}$ accuracy in Example 5

| Trapezoidal Variants | f | g | $f^{(1)}$ | $f^{(2)}$ | I_1 | I_2 | I_3 | Total evaluations |
|----------------------|-----|-----|-----------|-----------|-------|-------|-------|-------------------|
| CT | 285 | 2 | 0 | 0 | 284 | 0 | 0 | 571 |
| ZCT | — | — | — | — | — | — | — | — |
| MZCT | — | — | — | — | — | — | — | — |
| AMCT | 15 | 2 | 0 | 14 | 14 | 14 | 0 | 59 |
| GMCT | 327 | 2 | 0 | 326 | 326 | 326 | 0 | 1307 |
| HaMCT | 27 | 2 | 0 | 26 | 26 | 26 | 0 | 107 |
| HeMCT | 189 | 2 | 0 | 188 | 188 | 188 | 0 | 755 |
| CMCT | 21 | 2 | 0 | 20 | 20 | 20 | 0 | 83 |

Table 13: Average CPU time (in seconds) to achieve $|\epsilon| \leq 10^{-5}$ in examples 1-5

| Trapezoidal Variants | Example 1 | Example 2 | Example 3 | Example 4 | Example 5 |
|----------------------|------------|------------|-------------|------------|------------|
| CT | 68.043837 | 12.821123 | 432.303629 | 364.293037 | 39.670771 |
| ZCT | 552.603703 | 153.984100 | 6469.382491 | — | — |
| MZCT | 28.010080 | 5.261296 | 27.353811 | — | — |
| AMCT | 14.760520 | 3.085717 | 14.702231 | 20.346118 | 7.468816 |
| GMCT | 14.929914 | 3.146952 | 16.340413 | 42.374740 | 203.371200 |
| HaMCT | 14.880674 | 3.230150 | 17.171850 | 46.938636 | 11.446324 |
| HeMCT | 14.782009 | 3.061632 | 15.484834 | 30.986400 | 105.331456 |
| CMCT | 14.773490 | 2.944814 | 13.170858 | 35.370088 | 9.399820 |

4. Conclusion

This study focused the development of new variants of trapezoid-type quadrature keeping track on the efficiency in terms of time and cost effectiveness for the RS-integral approximation. The derivative corrections have been utilized at the points which were averages of the limits of integration. The derivation of proposed rules was discussed along with proved theorems on the local and global applications, local and global truncation errors and reduction to conventional forms. An exhaustive numerical examination was conducted for the thorough performance evaluation of the previous and new quadrature by considering varying nature test RS- integrals from literature. The new quadrature enhance precision and accuracy of the previously existing quadrature. The numerical results on error drops, accuracy (orders observed computationally), execution times and computational overheads in all considered problems reflected encouraging behavior and application of the proposed quadrature over existing ones. Besides, we also highlighted the critical cases indicating natural limitations and usability of the used quadrature for the RS-integrals. The proposed quadrature appear to be efficient enhancements, both in terms of accuracy and computational cost, over the existing ones. The contributions of

this study can be useful in future studies focusing the fractional integration and solving integral and integro-differential equations with different weight functions.

References

- [1] R. L. Burden and J. D. Faires. *Numerical Analysis*. Brooks/Cole, Boston, MA, USA, 9th edition, 2011.
- [2] P. R. Mercer. Hadamard's inequality and trapezoid rules for the riemann-stieltjes integral. *Journal of Mathematical Analysis and Applications*, 344:921–926, 2008.
- [3] P. R. Mercer. Relative convexity and quadrature rules for the riemann-stieltjes integral. *Journal of Mathematical Inequalities*, 6:65–68, 2012.
- [4] W. Zhao and H. Li. Midpoint derivative-based closed newton-cotes quadrature. *Abstract and Applied Analysis*, 2013. Article ID 492507.
- [5] W. Zhao, Z. Zhang, and Z. Ye. Midpoint derivative-based trapezoid rule for the riemann-stieltjes integral. *Italian Journal of Pure and Applied Mathematics*, 33:369–376, 2014.
- [6] M. M. Shaikh, M. S. Chandio, and A. S. Soomro. A modified fourpoint closed midpoint derivative-based quadrature rule for numerical integration. *Sindh University Research Journal (Science Series)*, 48(2), 2016.
- [7] T. Ramachandran, D. Udayakumar, and R. Parimala. Geometric mean derivative-based closed newton-cotes quadrature. *International Journal of Pure and Engineering Mathematics*, 4:107–116, 2016.
- [8] T. Ramachandran, D. Udayakumar, and R. Parimala. Harmonic mean derivative-based closed newton-cotes quadrature. *IOSR Journal of Mathematics*, 12:36–41, 2016.
- [9] T. Ramachandran, D. Udayakumar, and R. Parimala. Comparison of arithmetic mean, geometric mean and harmonic mean derivative-based closed newton-cotes quadrature. *Progress in Nonlinear Dynamics and Chaos*, 4:35–43, 2016.
- [10] T. Ramachandran, D. Udayakumar, and R. Parimala. Heronian mean derivative-based closed newton-cotes quadrature. *International Journal of Mathematical Archive*, 7:53–58, 2016.
- [11] T. Ramachandran, D. Udayakumar, and R. Parimala. Centroidal mean derivative-based closed newton-cotes quadrature. *International Journal of Science and Research*, 5:338–343, 2016.
- [12] Sara Mahesar, Muhammad Mujtaba Shaikh, Muhammad Saleem Chandio, and Abdul Wasim Shaikh. Some new time and cost efficient quadrature formulas to compute integrals using derivatives with error analysis. *Symmetry*, 14(12):2611, 2022.
- [13] Kashif Memon, Muhammad Mujtaba Shaikh, and Sara Mahesar. Numerical investigation of a four-point simpson's quadrature for computing riemann-stieltjes integrals. *NED University Journal of Research*, 22(1/2):27–44, 2025.
- [14] Kashif Memon, Muhammad Mujtaba Shaikh, Kamran Malik, Muhammad Saleem Chandio, and Abdul Wasim Shaikh. Efficient derivative-based simpson's 1/3-type scheme using centroidal mean for riemann-stieltjes integral. *Journal Of Mechanics Of Continua And Mathematical Sciences*, 16(3):69–85, 2021.

- [15] Weijing Zhao and Zhaoning Zhang. Simpson's rule for the riemann-stieltjes integral. *Journal of Interdisciplinary Mathematics*, 24(5):1305–1314, 2021.
- [16] Mohammad Alomari. A companion of ostrowski inequality for the stieltjes integral of monotonic functions. *Innovative Journal of Mathematics (IJM)*, 1(2):18–29, 2022.
- [17] Abdulrahman Obaid Alshammari, Muhammad Nawaz Khan, and Imtiaz Ahmad. Boundary layer challenges: a comparative analysis of two efficient meshless approaches. *Partial Differential Equations in Applied Mathematics*, 10:100743, 2024.
- [18] Shakeel Mehnaz, Muhammad Nawaz Khan, Imtiaz Ahmad, Sayed Abdel-Khalek, Ahmed Mohammed Alghamdi, and Mustafa Inc. The generalized time fractional gardner equation via numerical meshless collocation method. *Thermal Science*, 26(Spec. issue 1):469–474, 2022.
- [19] G. L. Bullock. A geometric interpretation of the riemann-stieltjes integral. *The American Mathematical Monthly*, 95(5):448–455, 1988.
- [20] W. Zhao, Z. Zhang, and Z. Ye. Composite trapezoid rule for the riemann-stieltjes integral and its richardson extrapolation formula. *Italian Journal of Pure and Applied Mathematics*, 35:311–318, 2015.
- [21] M. H. Protter and C. B. Morrey. *A First Course in Real Analysis*. Springer, New York, NY, 1977.
- [22] K. Memon et al. A modified derivative-based scheme for the riemann-stieltjes integral. *Sindh University Research Journal (Science Series)*, 52(1), 2020.
- [23] R. G. Bartle. *The Elements of Real Analysis*. John Wiley & Sons, 2nd edition, 1964.
- [24] Kashif Memon, Muhammad Mujtaba Shaikh, MS Chandio, and AW Shaikh. Heronian mean derivative-based simpson's-type scheme for riemann-stieltjes integral'. *Journal Of Mechanics Of Continua And Mathematical Sciences*, 16(3):55–68, 2021.
- [25] F. Zafar, S. Saleem, and C. O. E. Burg. New derivative-based open newton-cotes quadrature rules. *Abstract and Applied Analysis*, 2014, 2014. Article ID 109138, 16 pages.